

# TESSERAL GEO MODELING



## Modeling Applications in Seismic Case Studies

### Contents

1	Modeling of Velocity Quasi-Anisotropy .....	1
2	Modeling of effect of the upper part cross-section and surface relief .....	18
3	Studying of the near salt dome deposits .....	23
4	Testing of the seismic data processing programs.....	34
4.1	Multiple waves subtraction with the Born dissipation rows.....	34
4.2	Effect of the procedure of multiple wave subtraction on the velocity analysis .....	36
4.3	Programs of attenuation of the surface hindrance-waves .....	37
4.4	Survey layout parameters and AVO processing .....	38
	Summary .....	41
	References.....	43

## 1 Modeling of Velocity Quasi-Anisotropy

... effects connected with the thin-layering of the geological medium, which are of importance in the studying of mid-horizons thicknesses.

The effect of quasi-anisotropy – is one of the most wide spread in the practice of low frequency (10-100 Hz) seismic prospecting. If not taken into account it can frequently distort our understanding of the geological medium structure. For example, influence of quasi-anisotropy on AVO-effect is widely known. As it is shown in pares [1,2,3 and other], AVO-effect can be obtained not only due to the jump of the Poisson coefficient on the layers boundary, but also from the difference in the medium anisotropy parameters. This can either increase or attenuate (eradicate) AVO-effect. The indicated difference in the anisotropy parameters, as a rule, is caused by different cycles in thin-layered deposits, i.e. it has by its nature quasi-anisotropy [4]. Along with this, up to now we don't have simple solutions for recognizing quasi-anisotropy. That is why recognition of the influence on the studied seismic parameters is significantly complicated. It is important to notice that modeling of quasi-anisotropy in combination with other effects, typical to thin-layered medium, for example, interferential waves [5], by other methods (specifically ray-tracing), meet significant and sometimes undefeatable difficulties. Combination of the indicated effects is impossible to model, for example, on the basis of acoustic equation.

The simplest medium, characterized by quasi-anisotropic properties, is the periodical thin-layered model. Thin-layered periodical medium in condition that the wave length  $\lambda \gg d$ , where  $d$  – thickness of the thin layer, is well described by transversal isotropic model, characterized by

elasticity tensor with five elastic constants. If Lamé parameters are described in periodical medium by  $\lambda_1, \lambda_2, \mu_1, \mu_2$  and layers thickness as  $d_1$  и  $d_2$ , we obtain meaning of elastic parameters, with which we will be operating,  $C_{11}$  и  $C_{33}$ . They are responding to compressional velocities along ( $\alpha_{\parallel}$ ) and cross ( $\alpha_{\perp}$ ) layering, which correspondingly will be equal to:

$$C_{11} = \frac{1}{D} \{ (d_1 + d_2)^2 (\lambda_1 + 2\mu_1)(\lambda_2 + 2\mu_2) + 4d_1d_2(\mu_1 - \mu_2)[(\lambda_1 + \mu_1) - (\lambda_2 + \mu_2)] \} \quad (1a)$$

$$C_{33} = \frac{1}{D} (d_1 + d_2)^2 (\lambda_1 + 2\mu_1)(\lambda_2 + 2\mu_2), \quad (16)$$

where  $D = (d_1 + d_2)[d_1(\lambda_2 + 2\mu_2) + d_2(\lambda_1 + 2\mu_1)]$ .

As it can be seen from (1) condition of  $C_{11} \neq C_{33}$  is possible only for an elastic model when  $\mu_1$  and  $\mu_2$  are not equal to zero. For an acoustic model, as it will be shown below, in the case of periodical thin-layered pack the velocities are characterized by the circle indicatrice, i.e. quasi-anisotropy is absent.

Let us show examples of modeling the velocities with quasi-anisotropy. Physical adequacy of modeled effects, connected with the thin layering, is not evident by itself. It depends on a used mathematical model, exactness of the wave equation approximations with fine differences etc. That is why proof of the indicated adequacy is an important problem, directed to a wider application of modeling tools in the seismic practice.

For modeling quasi-anisotropy effect thin-layered model 1 was used, presenting a periodical interchange of layers with thickness 10 m and compressional velocities (P- waves)  $\alpha_1 = 2000$  m/s and  $\alpha_2 = 4000$  m/s, shear wave velocities (SV - waves)  $\beta_1 = 1150$  m/s and  $\beta_2 = 2310$  m/s and densities  $\rho_1 = 2.01$  g/cm<sup>3</sup> and  $\rho_2 = 2.35$  g/cm<sup>3</sup>. Thin-layered pack with  $h_1=500$ m (for modeling of vertical seismic profiling (VSP) shotgathers) and  $h_2 = 1150$ m (for modeling surface shotgathers) is underlain by a homogeneous layer with velocities  $\alpha_3 = 5000$  m/s,  $\beta_3 = 2900$  m/s,  $\rho_3 = 2.5$  g/cm<sup>3</sup>. Slightly outraged parameters of a periodical pack are chosen to obtain a more highlighted effect of quasi-anisotropy.

Modeled here are shotgathers of longitudinal (shot point coordinate  $X_s=0$ m) and transversal ( $X_s = 400$ m) VSP in variant of two-component receiving in the frequency band 10 Hz – 60 Hz. Z-component and X-component for transversal VSP is shown in Fig.1.

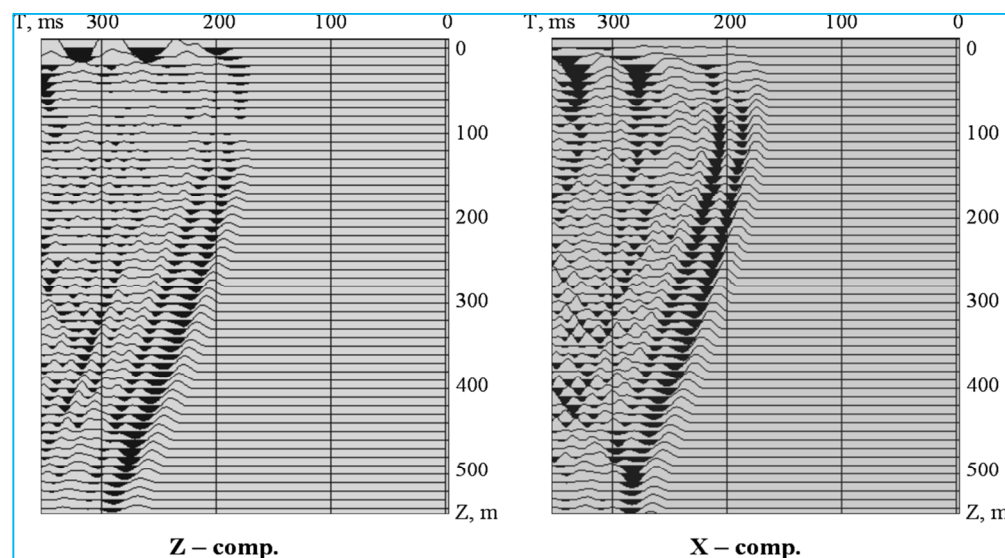


**Fig.1.** Transversal VSP shotgathers.

Wave field, obtained for a nearer source point, as a rule, is used for finding propagation velocity (P-waves) for normal incidence of waves on discontinuity. In this case interval velocity, obtained by averaging on base 100m, is approximately equal 2500 m/s. Theoretical normal velocity of low-frequency seismic approximation, calculated on the basis of expression (16), taking into account that:

$$\alpha_{\perp} = \sqrt{\frac{C_{33}}{\bar{\rho}}},$$

Where  $\bar{\rho}$  - average density of a thin-layered pack, corresponds to  $\alpha_{\perp} = 2470$  m/s, that is very close to the one defined in the model. Here the average velocity, which can be related to low frequency approximation, is equal  $\alpha_{avr} \approx 2667$  m/s. Such velocity for the indicated model could be obtained, for example, by the averaging of the sonic logging data (SL) within the thin-layered pack. In this case, the difference in SL and VSP velocities is connected not with velocities dispersion, observed in absorbing non-elastic medium, but with quasi-anisotropy. It can bring erroneous results if were not taken into account at definition of the attenuation parameters on the basis of studying of differences in SL and VSP velocities [6].

Using dispersion equation [7]

$$Q = \frac{1}{\pi} [\alpha_{vsp} / (\alpha_{aw} - \alpha_{vsp})] \ln(f_{AW} / f_{VSP}), \quad (2)$$

Where  $Q$  – quality,  $\alpha_{vsp}$ ,  $\alpha_{sl}$  – compressional wave velocities, defined with VSP and SL correspondingly,  $f_{vsp}$ ,  $f_{sl}$  – frequencies of seismic signal at SL and VSP, and accepting dominant frequency of incoming VSP impulse as 40 Hz, and SL – 15 KHz, we obtain estimation of a quality for this example at a level  $Q = 20$ . A priory was implemented elastic model, but medium with such quality can be related to absorbing one. This example shows that corrections to VSP velocity, defined with modeling SL data, can be later applied for obtaining non-distorted parameters of absorption using the difference in VSP and SL velocities.

Transversal VSP allows studying other properties of anisotropic medium, particularly, relating to different directions of polarization and slowness vectors. First corresponds to direction of oscillation of the medium particles, second – to direction of wave propagation. In isotropic medium, those directions coincide, and their difference indicates anisotropy.

To prove that in a given frequency band the medium behaves as quasi-anisotropic, incident waves were defined at angles of incidence towards vertical polarization vectors  $\varphi_i$  and vector of the wave front propagation (slowness vector) –  $\varphi_f$ , as functions of receiver depth.

To define angle  $\varphi_i$  standard methodic of VSP polarization method [8] was used. To define angle  $\varphi_f$  methodic was used, based on finding the slowness vector by the observation data from three excitation points that is applicable for horizontally layered medium.

Let excitation be done from three points A, B, and C, placed at distance  $\Delta x$  from each other. For calculation of the slowness vector in condition of the horizontally layered medium, it is necessary to use such dependency:

$$\varphi_f = \arctg((\partial t_x / \partial x) / (\partial t_z / \partial z)),$$

Where  $\partial t_x$  - increment of time in the well point with coordinate  $Z_0$  with excitation in points A and C,  $\partial x = 2\Delta x$ ,  $dt_z$  - time increment on the base  $\partial z$ , symmetrical relating to point  $Z_0$  for excitation in point B.

In Fig.2 are shown graphics of dependency  $\varphi_i = F(z)$  и  $\varphi_f = \psi(z)$ . As it can be seen from indicated figure, angle  $\varphi_f$  systematically is lower of angle  $\varphi_i$ . Difference in angles reaches  $8^\circ - 9^\circ$ , that can be explained by velocities anisotropy.

Tesseral package gives the user the unique possibility to follow the seismic wave fronts propagation with sequences of wave field snapshots, obtained in fixed moments of time. Shown on example of model 1, how with help of this functionality it is possible to prove by condition of  $\alpha_{\perp} \neq \alpha_{\parallel}$  a presence of quasi-anisotropy in the thin-layered pack.

In Figure 3, is shown the front of propagation of P – wave for model 1 at different times  $t = \text{const}$ . The shape of indicated front is close to ellipse, but as it will be shown below, it is not an ellipse, which is very important from the viewpoint of studying transversally isotropic media. Using known spatial position of the wave front in fixed time, it is possible to calculate velocity  $\alpha_{\parallel}$ , estimation of which, in this case is close to  $\alpha_{\parallel} = 3150$  m/s at theoretical  $\alpha_{\parallel} = 3156$  m/s. From this follows, first – high degree of coincidence of model and theoretical velocities, and secondly – a proof of condition  $\alpha_{\perp} \neq \alpha_{\parallel}$ .

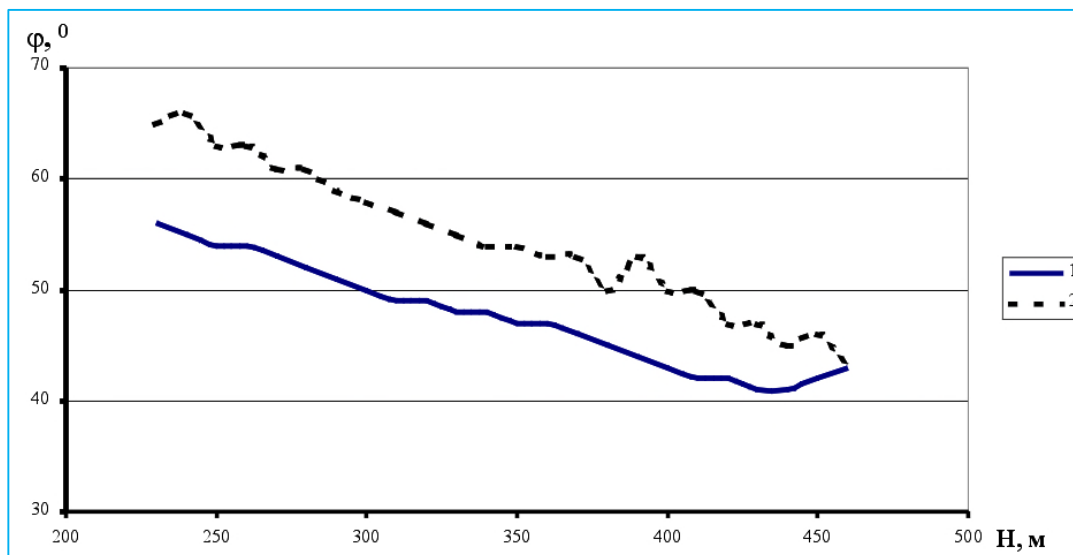


**Fig.2.** Charts of dependency of the slowness vector (1) and polarization vector (2) of incident wave from depth.

Tesseral modeling package provides other capabilities for the estimation of wave propagation velocities along layering.

Fig. 3 shows an example of determining velocity  $\alpha_{\parallel}$  towards the head wave propagation front. To create conditions of head wave appearance model 2 was used. In contrast from model 1 in the upper part of the model was inserted homogeneous layer with velocity  $\alpha_1 = 2000$  m/s and thickness  $h = 590$  m.

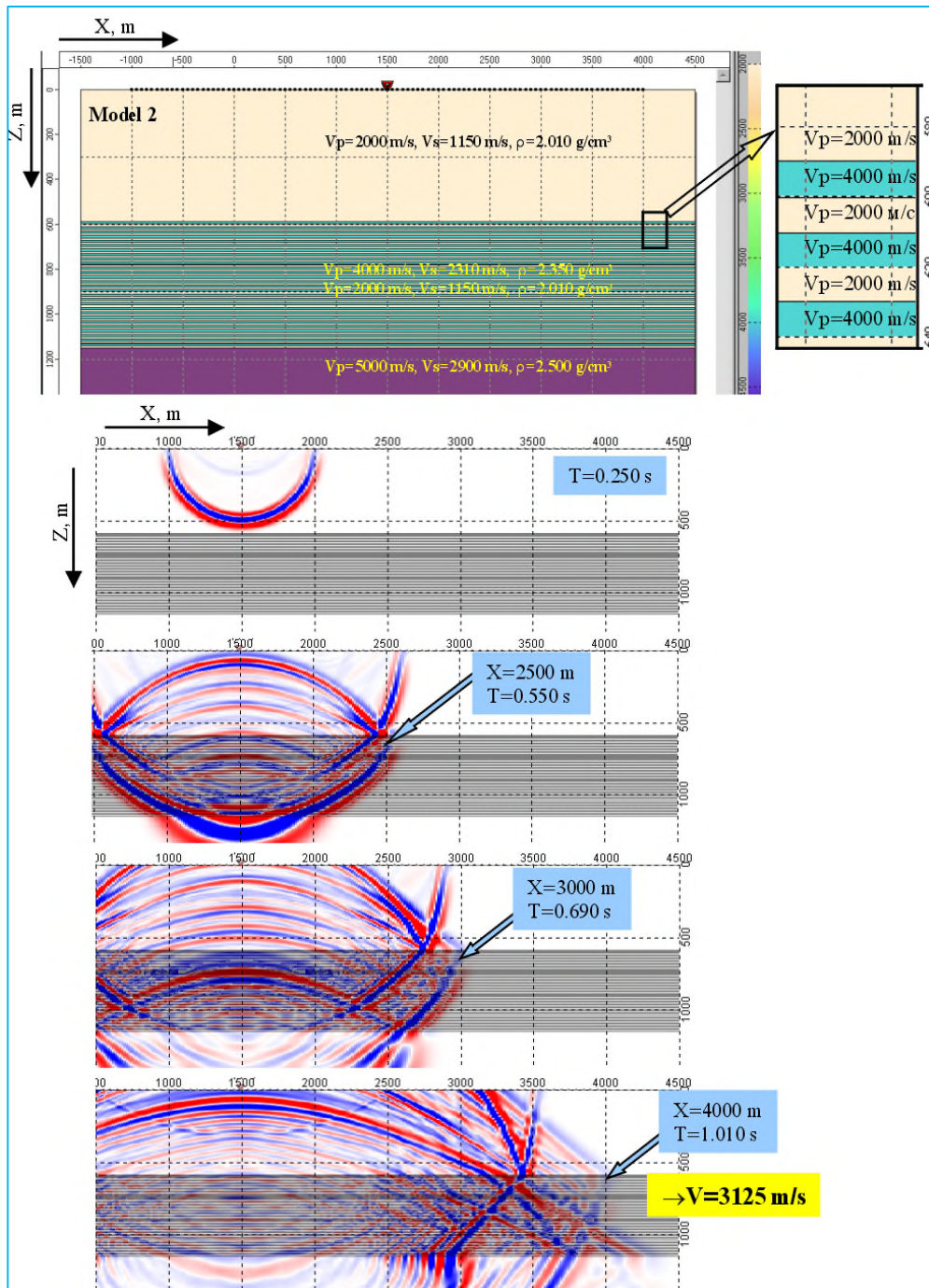


**Fig.3.** Determining of velocity  $\alpha_{\parallel}$  for elastic model 2 by the propagation front of the head wave, at fixed in time:  $t_1=0.250$  s;  $t_2=0.550$  s;  $t_3=0.690$  s;  $t_4=1.010$  s.

Fig.4 shows time sections of the wave field for times  $t = 0.55$  s,  $t = 0.69$  s and  $t = 1.01$  s correspondingly. For indicated sections of the wave front of propagation the head wave along horizontal discontinuity is well seen, its velocity, calculated by indicated sections is  $\alpha_{\parallel} = 3125$  m/s, is quite close to the theoretical  $\alpha_{\parallel} = 3156$  m/s.

The head wave, propagating in the upper layer, has an angle of incidence towards the horizontal direction  $\varphi \approx 39^\circ$ , that also allows calculation of the velocity of its propagation in the lower layer. In correspondence with the Snellius law for the head wave

$$\alpha_{\parallel} = \frac{\alpha_1}{\sin \varphi} \approx 3178 \text{ m/s}.$$

Here it is taken into account that  $\alpha_1 = 2000 \text{ m/s}$ , and angle  $\varphi \approx 39^\circ$ . Relative error of velocity measurements with such method does not exceed 1%.

Velocities of SV-waves in practice, as a rule, are defined using converted waves. Specific to those waves, is that to determine their velocity by waves propagating in a normal direction towards discontinuity is practically impossible. With the absence of a source of SV-waves it is simpler to determine velocity  $\beta_{\parallel}$ , which in transversally isotropic medium is equal to  $\beta_{\perp}$ .

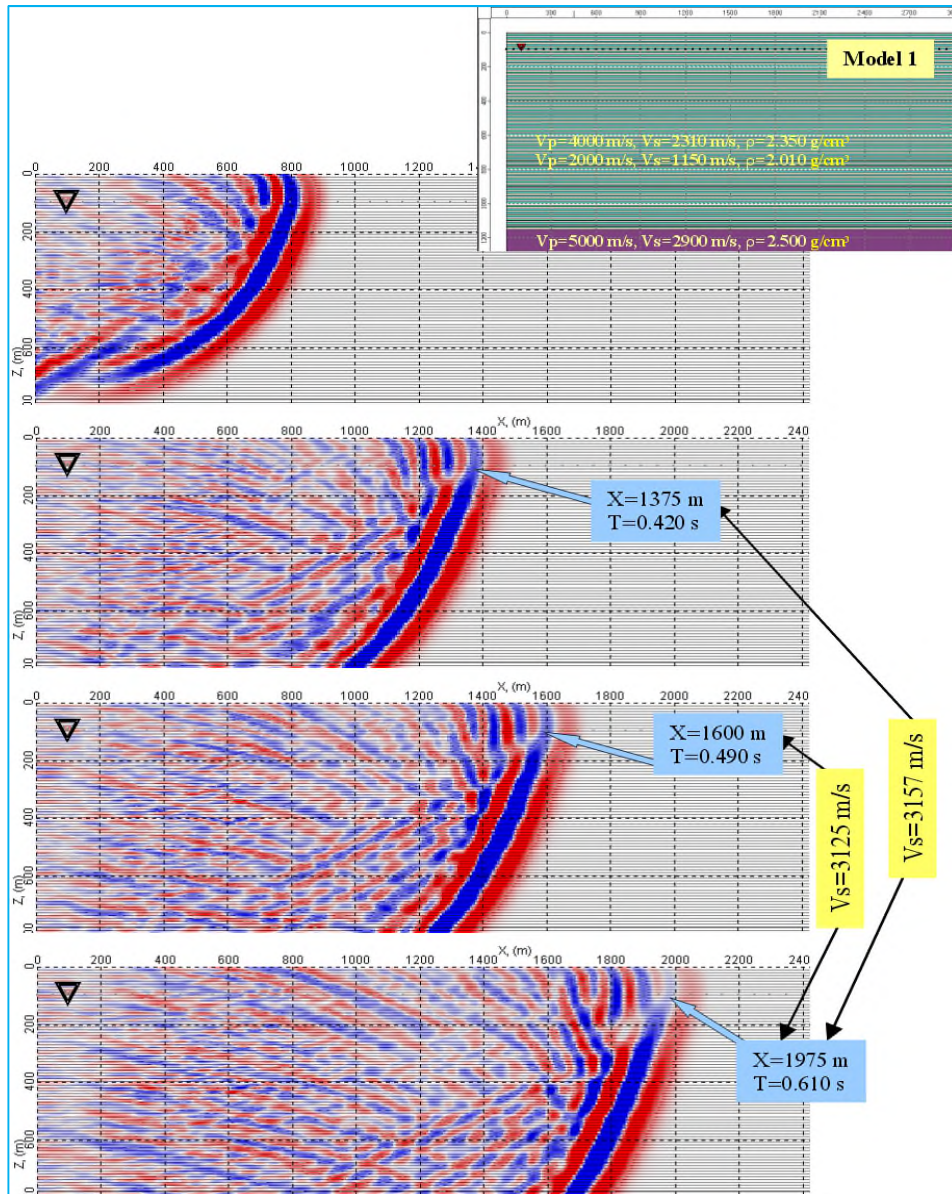


**Fig.4.** Fronts of P-wave propagation, obtained for elastic model 1 at fixed time:  $t_1=0.250 \text{ s}$ ;  $t_2=0.420 \text{ s}$ ;  $t_3=0.490 \text{ s}$ ;  $t_4=0.610 \text{ s}$ .

Fig. 5 shows an example of determining velocity  $\beta_{\parallel}$  of the converted head SV-wave basing on model 3. In this model, in distinction from model 2, for obtaining converted SV-wave, propagating over thin-layered pack, additionally included was the upper layer with thickness  $h = 200 \text{ m}$ , characterized by parameters  $\alpha = 1500 \text{ m/s}$ ,  $\beta = 900 \text{ m/s}$  и  $\rho = 1.97 \text{ g/sm}^3$ . Here the same method is applied as with the determining of velocity  $\alpha_{\parallel}$ , i.e. are used time sections of

the wave field at  $t_1 = 0.81$  s,  $t_2 = 1.11$  s,  $t_3 = 1.42$  s. Estimation of shear wave velocity along layering is  $\beta_{\parallel} \approx 1470$  m/s with the theoretical one  $\beta_{\parallel} = 1420$  m/s. Average velocity for given model, which could be obtained from wide-band sonic logging is  $\beta_{avr} = 1535$  m/s. As it is seen from given velocity values, finding of SV-waves absorption on the basis of the dispersion equation also requires the introduction of some correction.

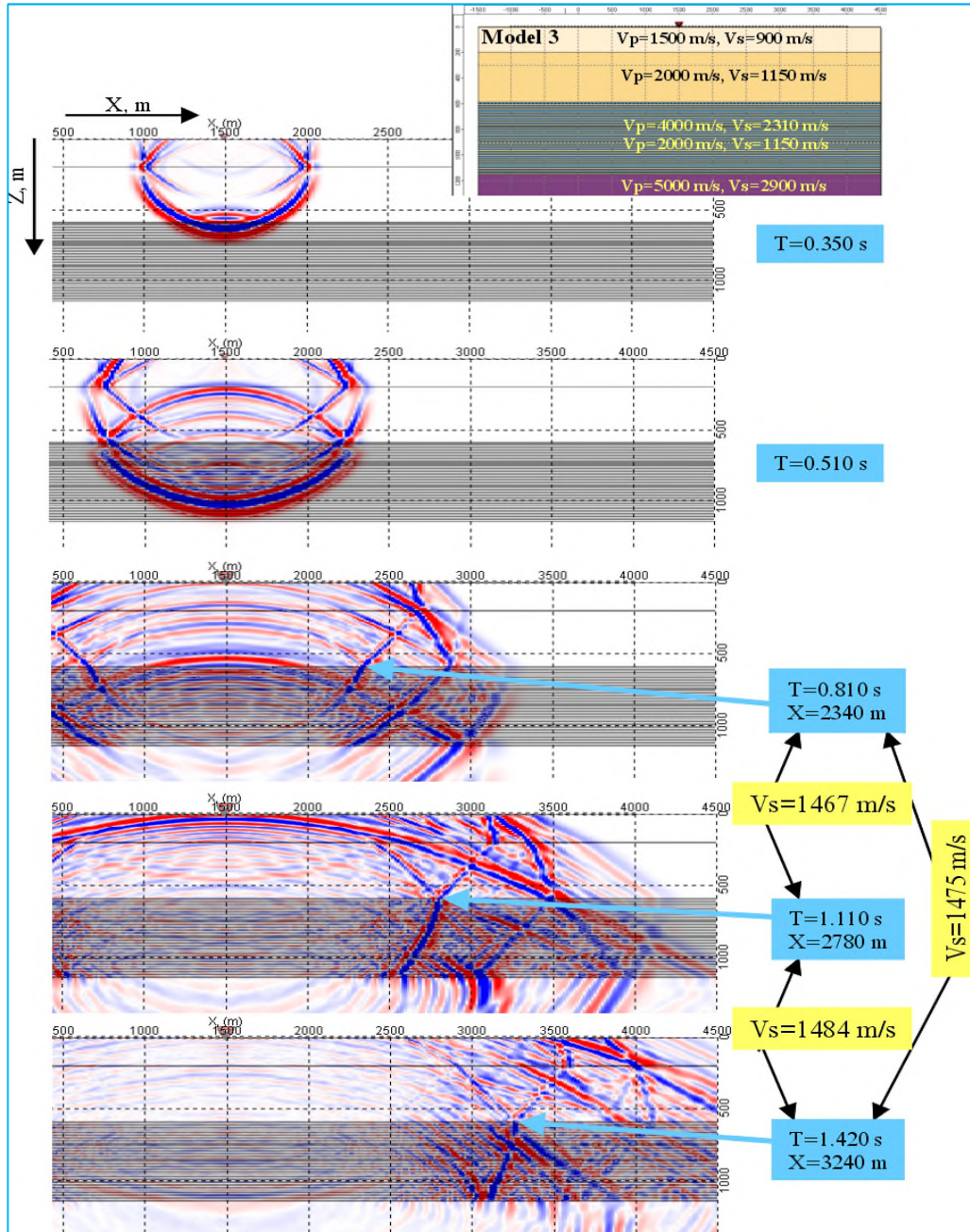


**Fig.5.** Determining of velocity  $\beta_{\parallel}$  for acoustic model 3 by front of the head wave propagation, at fixed in time:  $t_1=0.350$  s;  $t_2=0.510$  s;  $t_3=0.810$  s;  $t_4=1.110$  s;  $t_5=1.420$  s.

Demonstrated here the methodical approach has important practical significance for the detailed study of properties of mid-horizon thin-layered deposits, model of which is formed by acoustic and density well logging data.

In connection with the question about physical adequacy of modeling results, the studying of wave velocities propagating in a thin-layered pack, for the acoustic model would be important. As it was indicated above, in correspondence with expression (1) in this case  $C_{11} = C_{33}$ . Figure 6

shows time sections of wave field for model 2 calculated in acoustic approximation of the wave equation. Velocity of the head wave propagation in thin-layered pack in this case is close to  $\alpha_{\parallel} \approx 2440$  m/s, which practically corresponds to  $\alpha_{\perp}$ .

Anisotropy of P-waves in the case of an elastic medium leads to the velocity indicatrice, which can considerably differ from an ellipse. Distortion of ellipsicity of indicatrice depends from parameter [9]

$$\Delta\alpha(\theta) = \alpha_{\perp} (\delta - \varepsilon) \sin^2 \theta \cdot \cos^2 \theta, \quad (3)$$

where  $\delta$  and  $\varepsilon$  – Thompson parameters, defined by correspondences:

$$\varepsilon = \frac{C_{11} - C_{33}}{2C_{33}} \quad (4)$$

$$\delta = \frac{(C_{13} + C_{44})^2 - (C_{33} - C_{44})^2}{2C_{33}(C_{33} - C_{44})}.$$

In case  $\Delta\alpha(\theta) < 0$  P-waves velocity indicatrice is placed inside the ellipse, at  $\Delta\alpha(\theta) > 0$  – outside. This fact has crucial importance in the analysis of P-waves effective velocities, determined by the surface shotgathers.

In the case of the elliptical character of indicatrice  $\Delta\alpha(\theta) \approx 0$ , that occurs in real conditions for small values of  $\varepsilon = [0,01 \div 0,03]$  [3], effective velocity, determined by surface shotgathers,  $\alpha_{\text{eff}} = \alpha_{\parallel}$ . For  $\Delta\alpha(\theta) < 0$  effective velocity can be significantly lower  $\alpha_{\parallel}$  and even average square  $\alpha_{\text{asq}}$ . At this time in thick-layered media, a phenomenon of quasi-anisotropy is not appropriate,  $\alpha_{\text{eff}} \geq \alpha_{\text{asq}}$ . Parameter  $(\delta - \varepsilon)$ , determining value of  $\Delta\alpha(\theta)$  for this model is  $\delta - \varepsilon = -0.32$ , that presumes significant decreasing  $\alpha_{\text{eff}}$  relating to  $\alpha_{\parallel}$ . This is proved by the result of experimental measurement of effective velocity from the shotgather, obtained by model 1 (Fig.7) -  $\alpha_{\text{eff}} \approx 2600$  m/s at  $\alpha_{\text{asq}} = 2828$  m/s.

In the case of transforming the model into thick-layered by gathering all low velocity and high velocity layers in two separate layers (Fig.8) effective  $\alpha_{\text{eff}} \approx 2900$  m/s, i.e.  $\alpha_{\text{eff}} \approx \alpha_{\text{asq}}$ .

In such a way, medium, in which  $\alpha_{\text{eff}} < \alpha_{\text{asq}}$  is anisotropic and requires special investigation for determining velocity  $\alpha_{\perp}$ , used for transition from the isochronal maps to the depth maps. In practice,  $\alpha_{\text{asq}}$  can be defined by longitudinal VSP or SL data.

In practice significant interest represent sites, characterized by such medium parameters for which  $\alpha_{\text{eff}} < \alpha_{\perp}$ , where  $\alpha_{\text{eff}}$  – velocity defined by CDP shotgather. This case corresponds to condition of sharp cross-section differentiation by values of the Poisson coefficient, that in terrigene cross-section can indicate its saturation with gas.

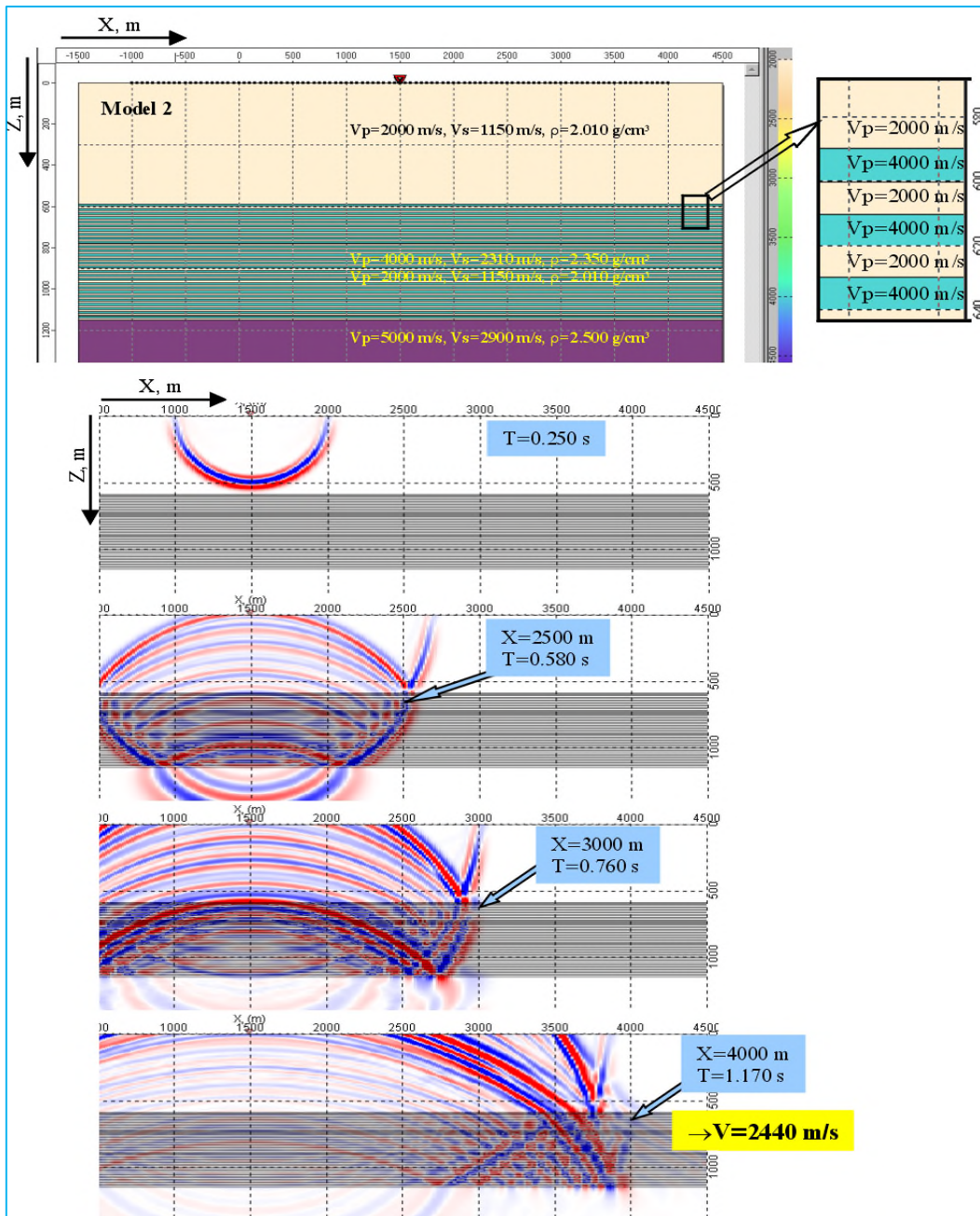


**Fig.6.** Determining of velocity  $\beta_{\parallel}$  for acoustic model 2 by the head wave propagation front, in fixed time:  $t_1=0.250$  s;  $t_2=0.580$  s;  $t_3=0.760$  s;  $t_4=1.170$  s.

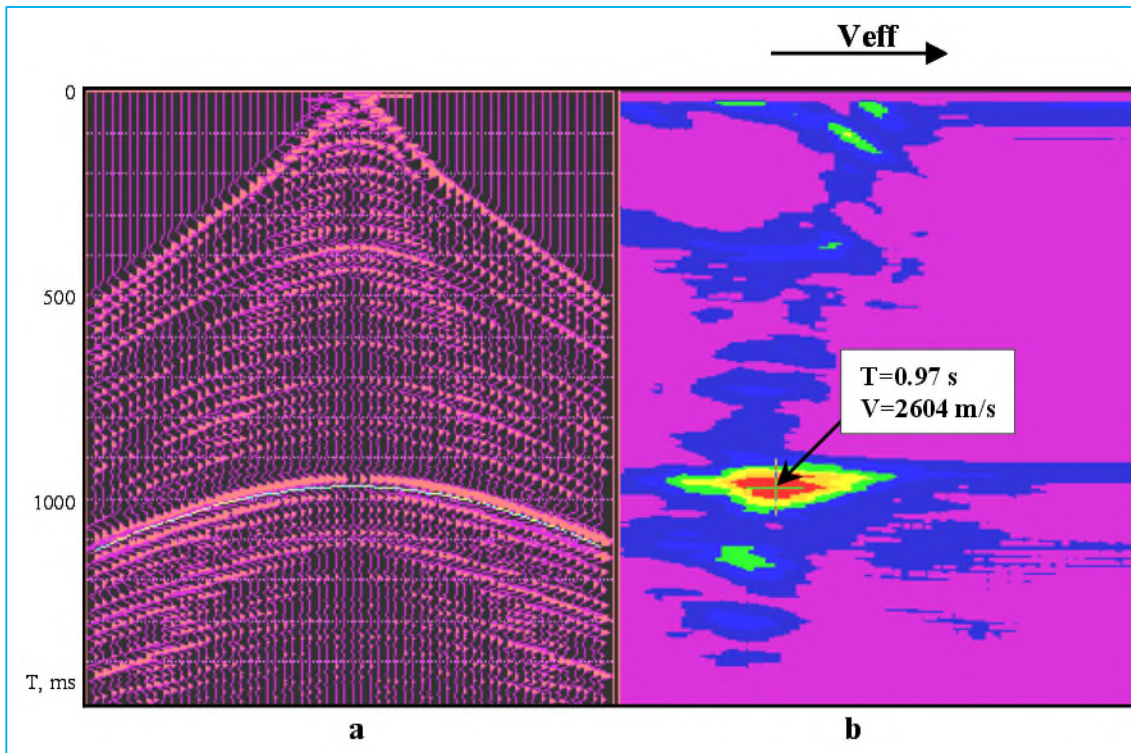


**Fig.7.** Determining of effective velocity by synthetic shotgather, obtained for thin-layered model: a – synthetic shotgather, b – vertical specter of velocity.

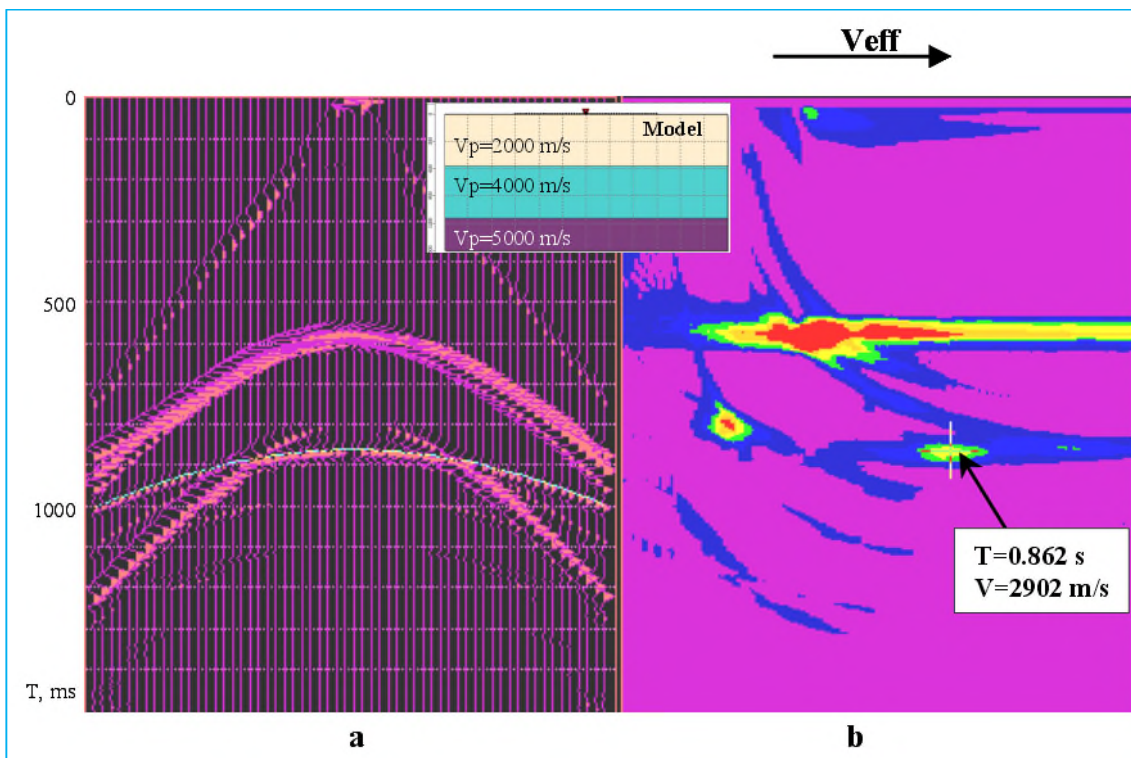


**Fig.8.** Determining of effective velocity by synthetic shotgather: a – synthetic shotgather, b – vertical specter of velocity.

Here is an example of the *Tesseral* modeling package for additional studying of indicated sites.

Well Sht-2 located on the Black See shelf is characterized by relation of VSP velocities (close to  $\alpha_{\perp}$ ) and CDP velocities (equal to  $\alpha_{eff}$ ), shown in fig.9, i.e.  $\alpha_{eff} < \alpha_{\perp}$ . Based on SL on compressional

waves, using approximating dependencies for density and shear wave velocities let consider model shown in fig.10f. Shotgather of longitudinal VSP, calculated for this model is shown in fig.10b. In fig.11 are shown interval velocities, defined in 100-meter floating intervals, for synthetic and real VSP shotgathers. From this figure it is seen, that the velocity of the real VSP (low frequency band) is considerably lower, than the velocity defined by the synthetic shotgather. Here, because of using modeling seismic frequency band, the mentioned above correction is already introduced. So, difference in velocities is determined, mainly by velocity dispersion, caused by non-elastic absorption. Applying for data shown in fig.11 formula (2), taking into account that  $f_{VSP}=25\text{Hz}$ ,  $f_{SL}=15\text{KHz}$ , we obtain  $Q = 4,4$ . The indicated level of quality, as a rule, characterizes intervals of cross-sections with considerable absorption and high probability of gas saturation. In the geologic relation – these are high-pored limestones. It is important to notice, that because of a low electrical resistance obtained from side well logging data, this interval was related to waver-saturated. After modeling, the well logging interpretation was revised, and low resistivity was explained by presence of tied water, that does not contradict gas-saturation.

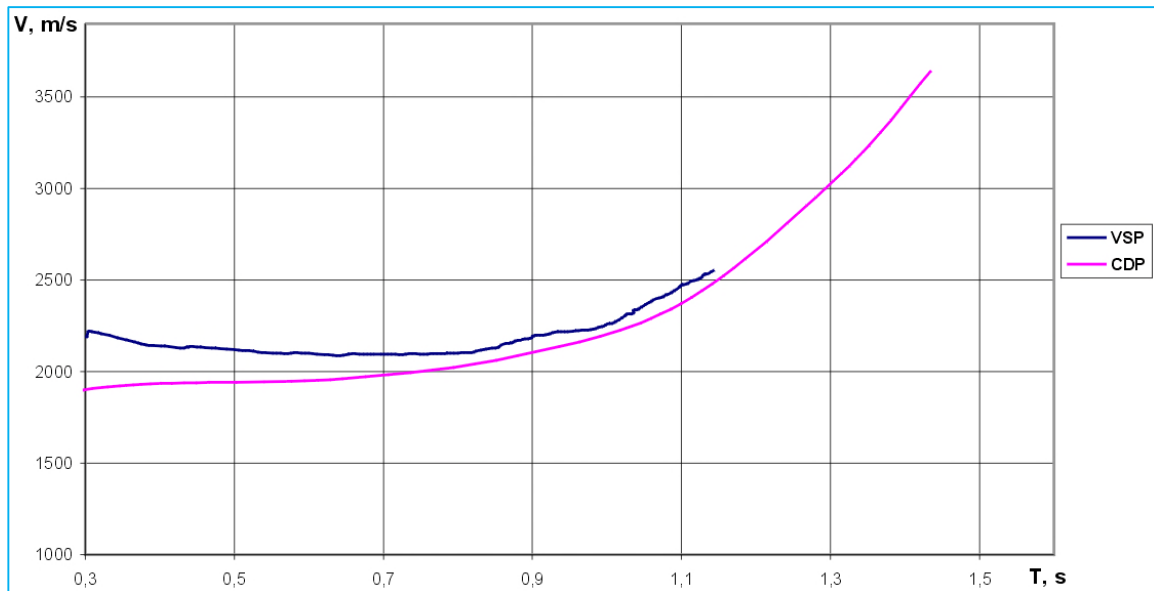


**Fig.9.** Charts of VSP and SDP velocities.

The next example will be relating to inverse correspondence of VSP and SL velocities, i.e. when first are higher than latter. Fig.12 shows the model, obtained by SL data on compressional waves for well II-2 located on the Black Sea shelf. In fig.12b is shown VSP shotgather, obtained based on the indicated model.

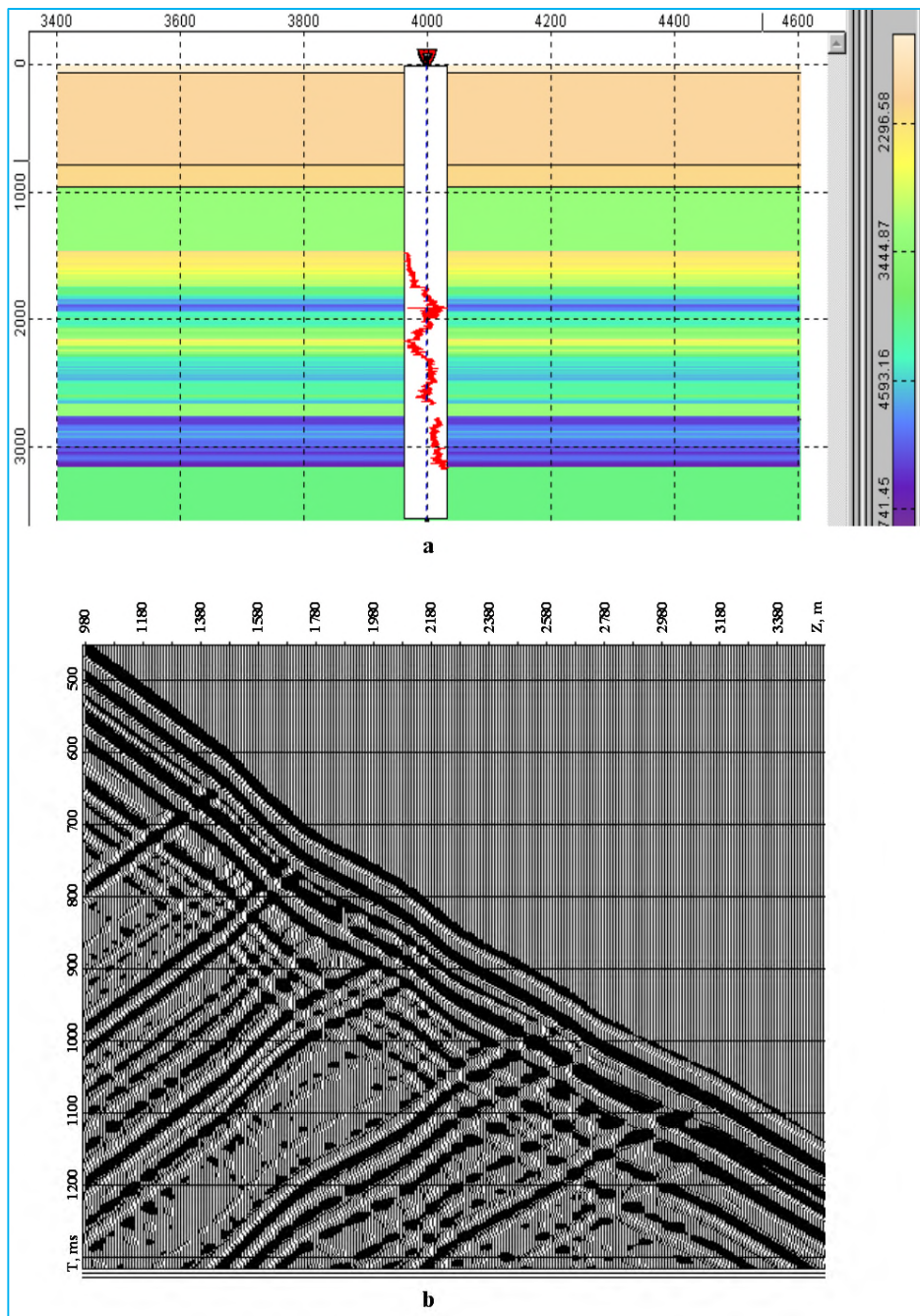


**Fig.10.** Model (a) of horizontally-laid thin-layered thickness, built by acoustic well-logging data of well Sht-2 and model VSP shotgather (b).

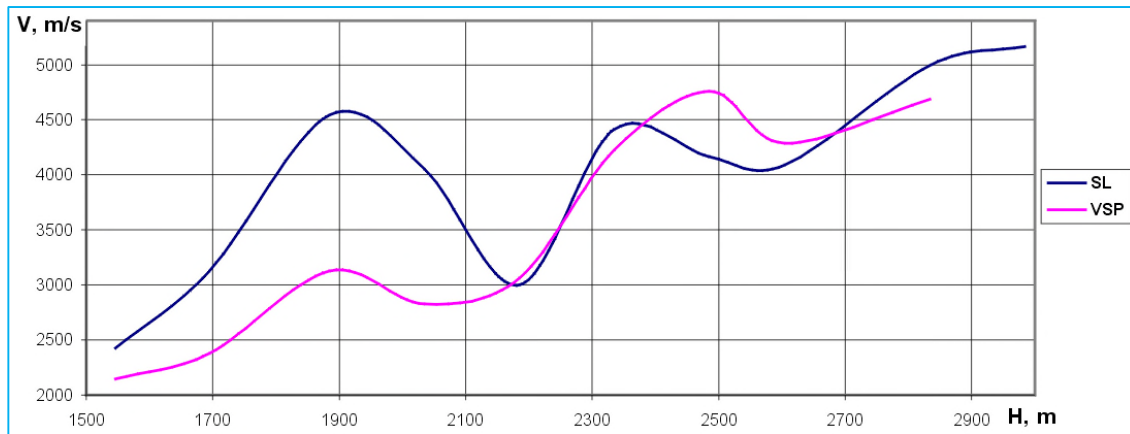


**Fig.11.** Charts of interval velocities, defined by model (SL) and real (VSP) shotgathers.

Considered is an interval of the cross-section (1200m-1700m), which is related to lower cretaceous effusive deposits and, despite horizontal layering of horizons, can be characterized by the angle of mid-horizon discrepancy, that is practically not revealed in the time cross-sections. This interval is characterized by such velocities:  $V_{SL}=4030$  m/s,  $V_{VSP}=4347$  m/s and the velocity determined by modeling is equal to  $V_{MOD}=3960$  m/s. Relation  $V_{SL} < V_{VSP}$ , as a rule, is caused by quasi-anisotropy in condition of inclined layered thickness, in this case, discrepant deposition of layers.

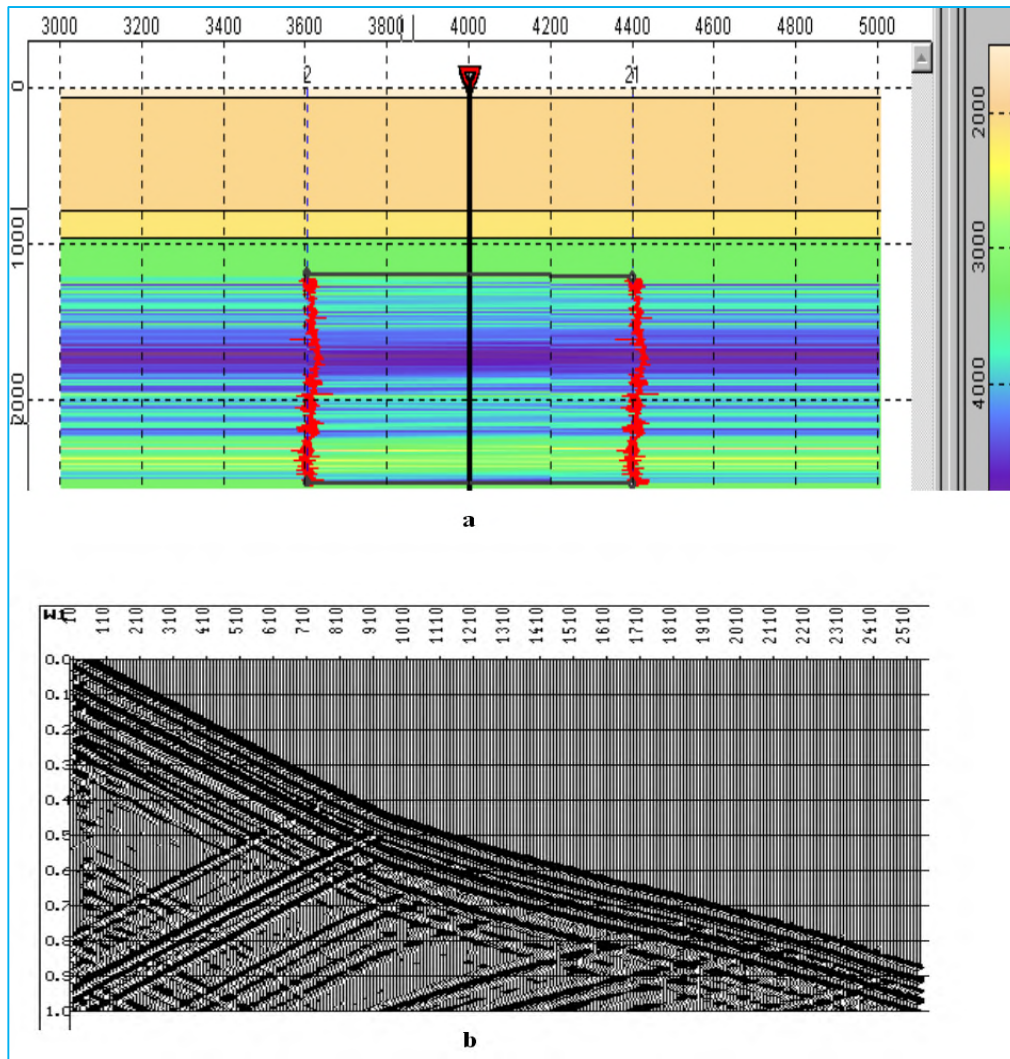
To determine the angle of indicated discrepancy, let the incline mid-horizon thickness be at an angle of  $30^\circ$ . For this the same LAS-file of sonic logging is used, placed in positions providing the indicated angle. The corresponding model is shown in fig.13a, obtained by it VSP shotgather is given in fig.13b. Velocity, calculated by this shotgather, in deposition the interval of low cretaceous effusives is equal to 4060 m/s, that is lower than velocity, determined by a real VSP shotgather.

Let incline with the same methodical approach mid-horizon thickness by an angle of  $50^\circ$ . The corresponding model is shown in fig.14a, obtained by it VSP shotgather is shown in fig.14b. Calculated by this, in the considered interval, velocity is equal to 4275 m/s, that only by 1.5% differs from the one of observed VSP shotgather. It allows supposing, that the inclination of effusive deposits is close to  $50^\circ$ .

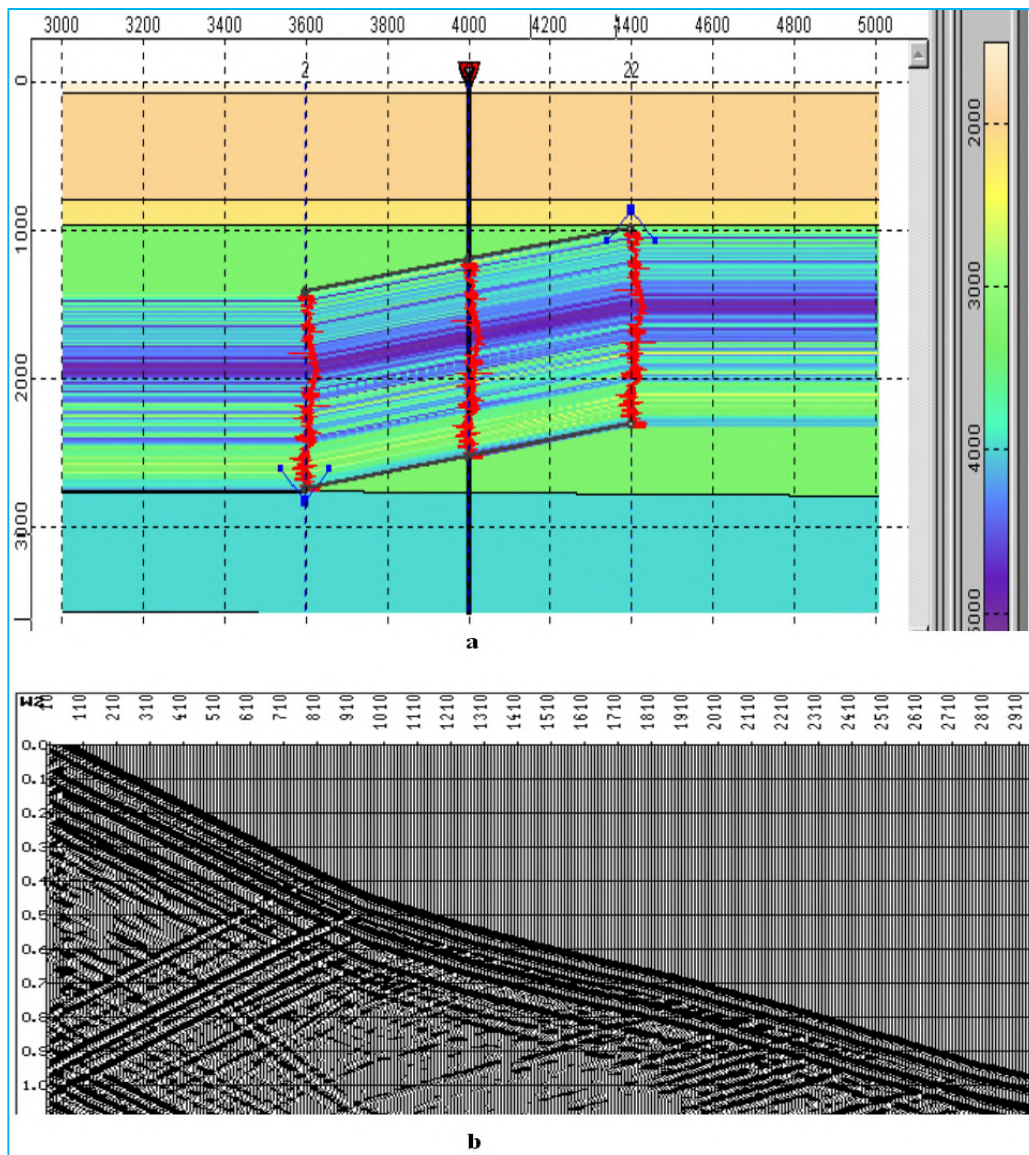
It must be indicated, that in this case, data about shear sonic and density logging were absent. In this situation, indicated data are taken from tables, presented in the *Tesseral* package. Presence of exact data about shear velocities and densities could in some degree change the obtained result.

One of the important functional advantages of the *Tesseral* package is the possibility of modeling thin-layered mediums, parameters of which are changing laterally. For this several wells with acoustic and density logs are used, located in one profile. Between wells, interpolation of parameters is conducted.

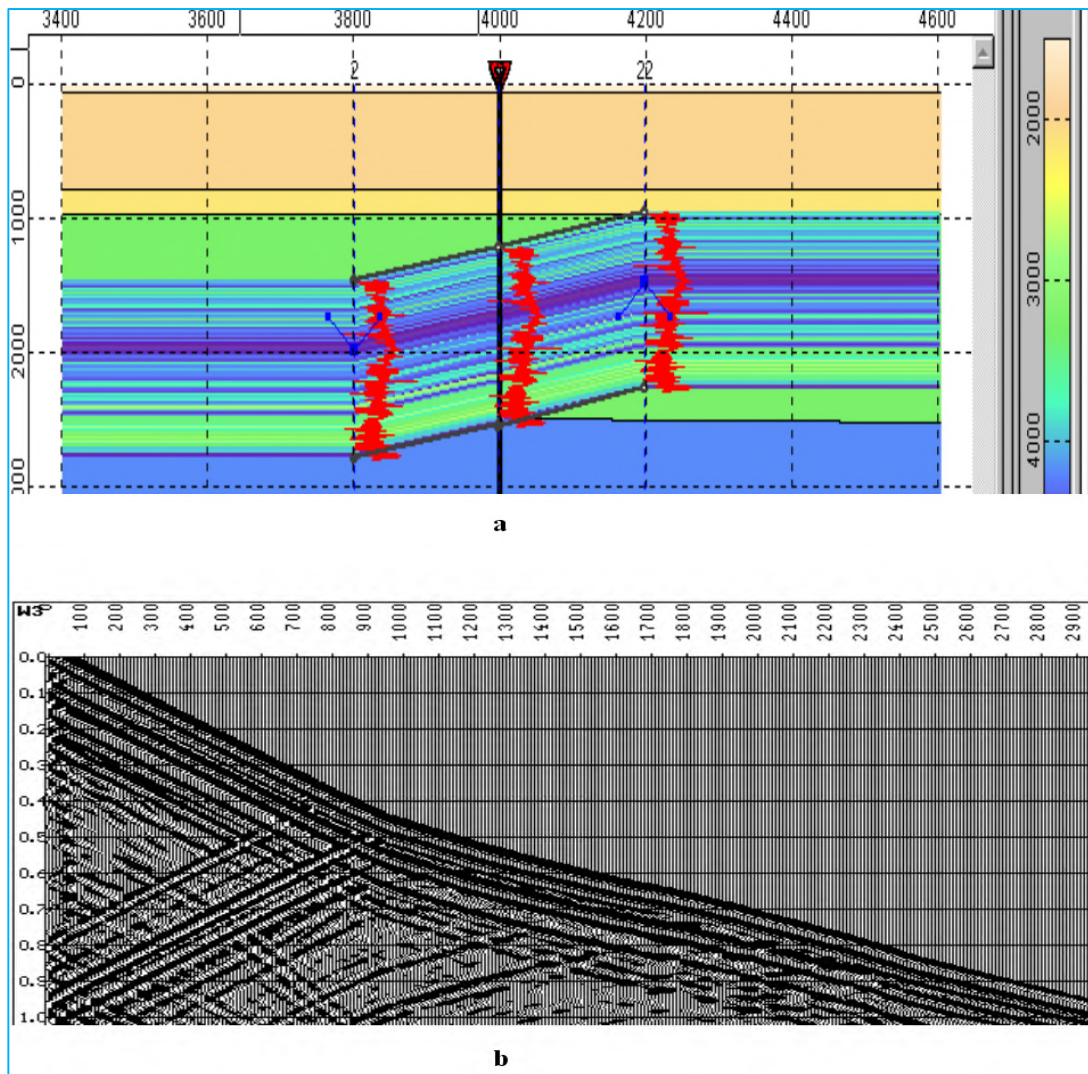
Fig.15a shows a model of the profile located within the area of the Black Sea shelf and built using sonic logging on compressional waves for four wells data. In indicated picture lateral medium heterogeneity is clearly seen (as color palette changes).



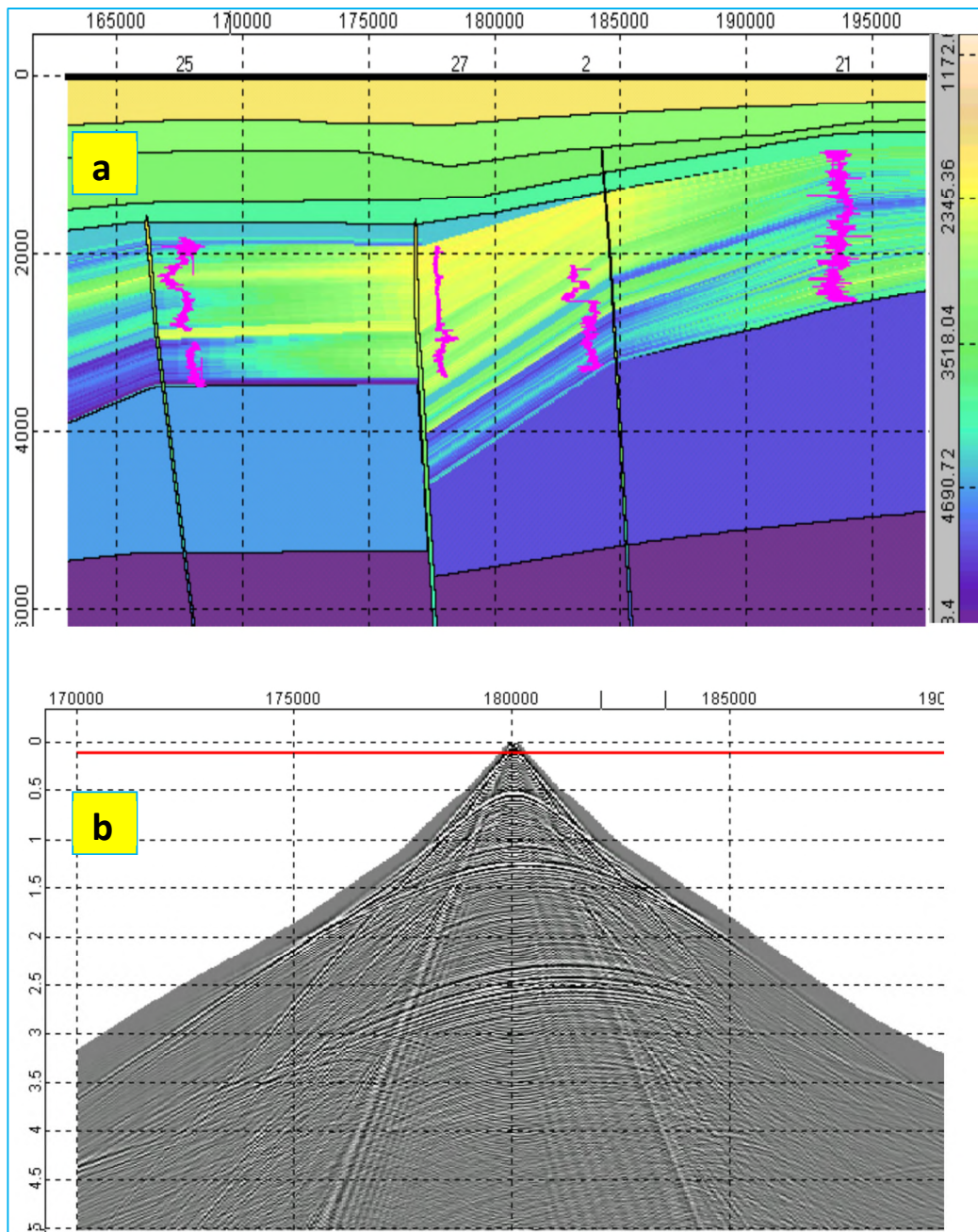
**Fig.12.** Model (a) of horizontally-laid thin-layered thickness, built by sonic log data of well II-2 and model VSP shotgather (b)



**Fig.13.** Modeling of VSP shotgather in condition of inclined thin-layered thickness, built by sonic log data of well II-2 by angle 30°: a – model; b – model VSP shotgather.



**Fig.14.** Modeling of VSP shotgather in condition of inclined thin-layered thickness, built by sonic log data of well II-2 by angle 50°: a – model; b – model VSP shotgather.



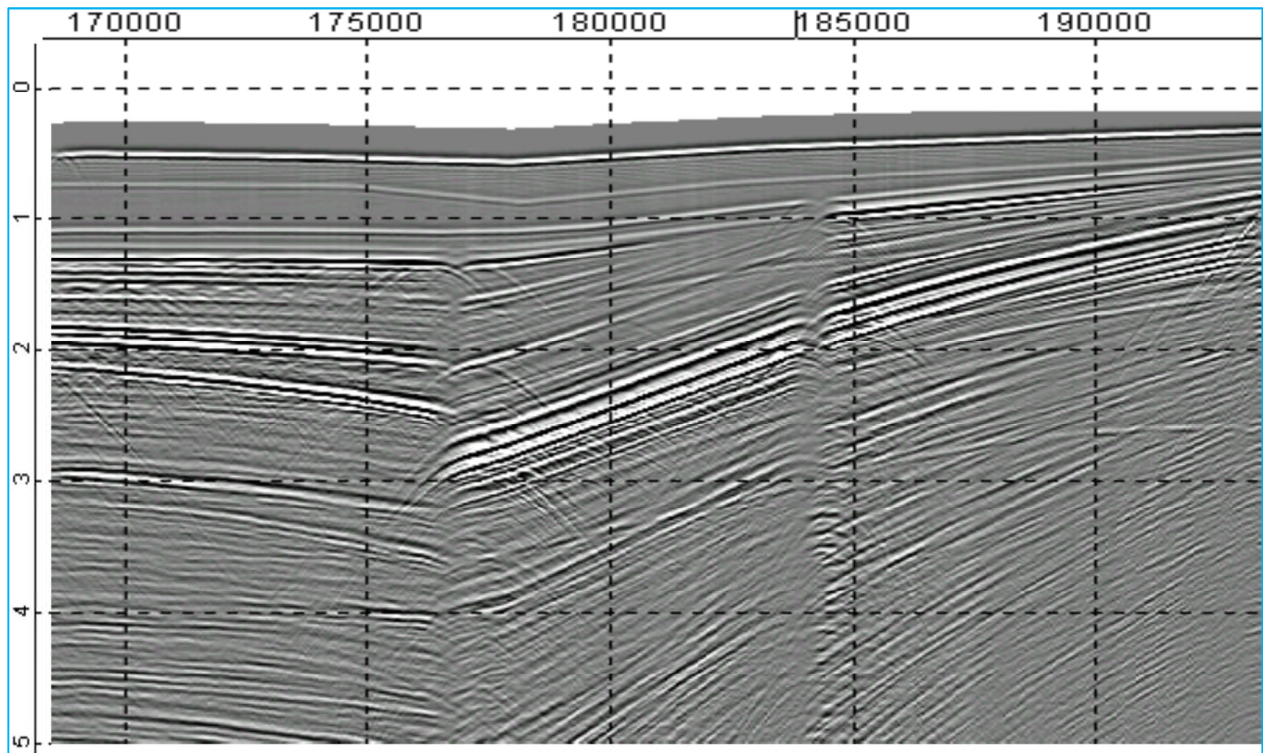
**Fig.15.** Modeling of wave field for lateral change of parameters of thin-layered deposits on example of profile located within the Black See shelf area: a – model; b – synthetic CDP shotgather.

Figure 15b shows a CDP shotgather, obtained from the given model, in which there are clearly seen effects, connected with inclined thin-layered packs.

Fig. 16 shows time cross-section, modeled in “exploding reflectors” mode. Thin-layering is revealed in multiple phasing of reflections. In this case reverberation waves were not modeled (was used option of “free surface absence”) and because of this, all multiple waves are connected with mid-layer reflections, the influence of which in this case is quite big.

In shown figure are clearly seen tectonic disruptions, that are the source of intensive diffracted waves, created on thin-layer boundaries.

Lateral change of velocities is displayed, partly, in synphasic axes of inclination on coordinates X=170000m – 177000m at horizontal reflecting boundaries.



**Fig.16** Time cross-section, obtained from model, shown in fig. 15a.

## 2 Modeling of effect of the upper part cross-section and surface relief

... taking into account of heterogeneities of the upper part of the cross-section (weathered layer) and unevenness of the observation surface and modeling their influence on the seismic wave fields.

Influence of the upper part of cross-sections on the quality of seismic materials is caused, mainly, by surface relief and differentiation of low-velocity zones (LVZ, weathered layer), within which are generated complexly polarized surface waves. The intensity of the latter can many times exceed intensiveness of useful reflected waves. This can even be true in a case when surface waves do not simply propagate as direct, but dissipate on different heterogeneities (relief unevennesses, disruptions, local lithological heterogeneities etc), transforming into the most effective regular hindrance. Possibilities of modeling with the *Tesseral* package of surface waves, particularly Releigh waves, allows for clear identification and more effective handling of indicated hindrances.

For modeling of seismic effects, connected with the upper part of the cross-section, creation of sufficiently detailed and precise LVZ models and surface relief are necessary.

As an example, consider data obtained from seismic profile 14 (Podleskovsky area of Dnieper-Donetsk depression (DDP), Ukraine). Fig.17 shows a velocity model of this profile, and in fig.18

in zoomed scale – the model of the upper part of the cross-section, built with micro-well logging data and tied to them vertical times, obtained with explosion type of source.

Fig.19 shows shotgathers of common shot point (CSP) for coordinate  $X=7000\text{m}$ , obtained as a result of fitting of the base of the receiver grouping. Calculation of the seismogram was done for the receiver interval  $\Delta X=5\text{m}$ , that allowed synthesis of real groups. As it can be seen from fig.19, optimal suppression of the surface waves occurs for the group length 150m. In this situation it is important to indicate sharp asymmetry of left and right shotgather branches. Within the shotgather limits in considerable degrees are suppressed reflected waves. Let investigate the cause of this phenomenon be the interference of the surface waves with the reflected ones. For this aim place well in the profile coordinate  $X=5500\text{m}$  and model Z- and X-components of VSP shotgather, shown in fig.20a and fig.20b correspondingly. In shotgather of Z-component in the low depth area (from 0m to 300m) are observed intensive waves with hyperbolic form of time-curve. Interference of them with the target reflected waves leads to practically full suppression of the latter ones at coming out to the surface. Taking into account that waves propagating in the upper part of the cross-section and having the main part of the energy in Z-component are transversally polarized; it can be presumed that they are Releigh surface waves. To prove this let model VSP shotgather in the same coordinate, but in the acoustic approximation of the wave equation. Corresponding Z- and X- components of the wave field are shown in fig.21a and 21b. As it can be seen from this figure, in Z-component intensive waves are not generated, that is explained by the impossibility of propagation of shear waves in the acoustic medium. In this case reflected waves without interference reach the surface. It can also be clearly seen in the CSP shotgather, modeled in acoustic approximation, shown in variant fitting of the grouping bases in fig.22. As it can be seen from the indicated figure, left and right branches of shotgathers practically do not differ from each other, that proves the absence in this case of the interference, connected with dissipated Releigh wave. Detailed investigations of this model show, that the indicated wave is dissipated on unevennesses of the relief, partly in “cut” shown in fig.18.

Time CDP cross-section ( $T_0$ ), formed for considered model (fig.17), is represented in fig.23. Targeted in this case are horizons of bashkir layer of middle Carbon, fixing at times  $t_0=2500-2800$  ms. within those horizons in the interval of points  $X=8200\text{m} - 8800\text{m}$  is observed considerable attenuation of the record intensiveness. It must be noticed, that similar attenuation is observed also in real data, and where basing on this in this place was predicted disruptive fracturing. The modeling done with full evidence shows, that indicated attenuation of the record intensiveness is connected with dissipated surface waves.

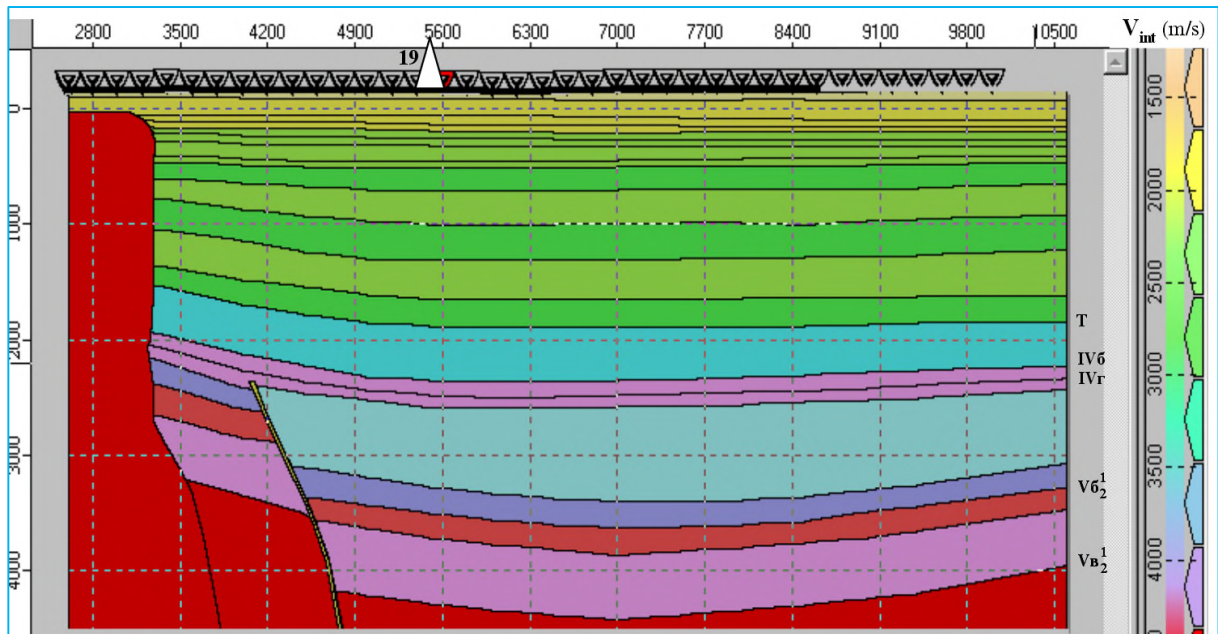


Fig.17. The medium velocity model.

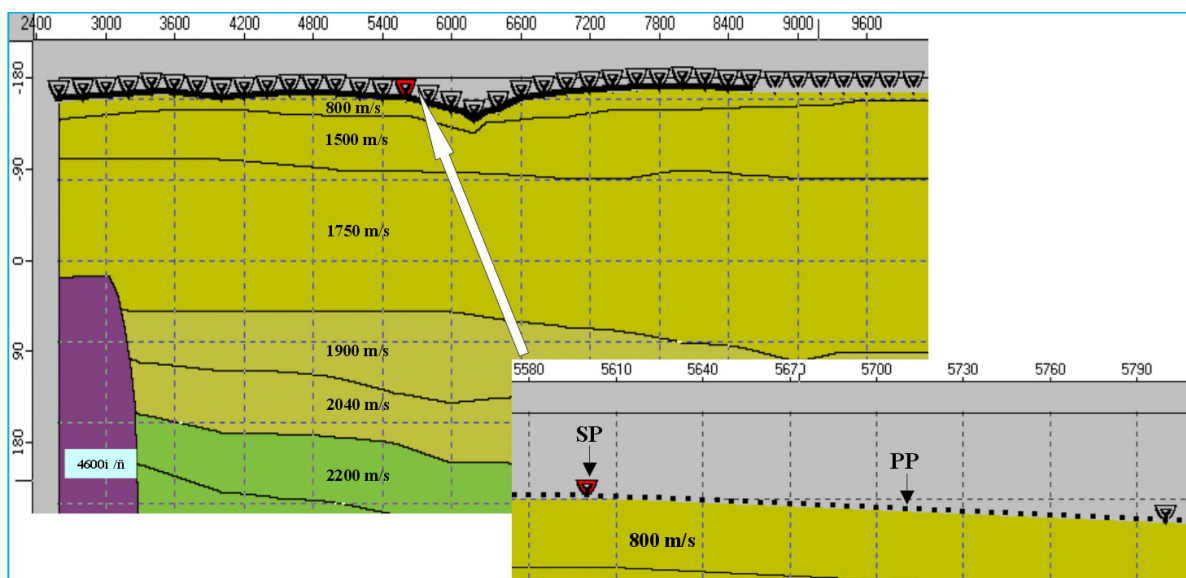
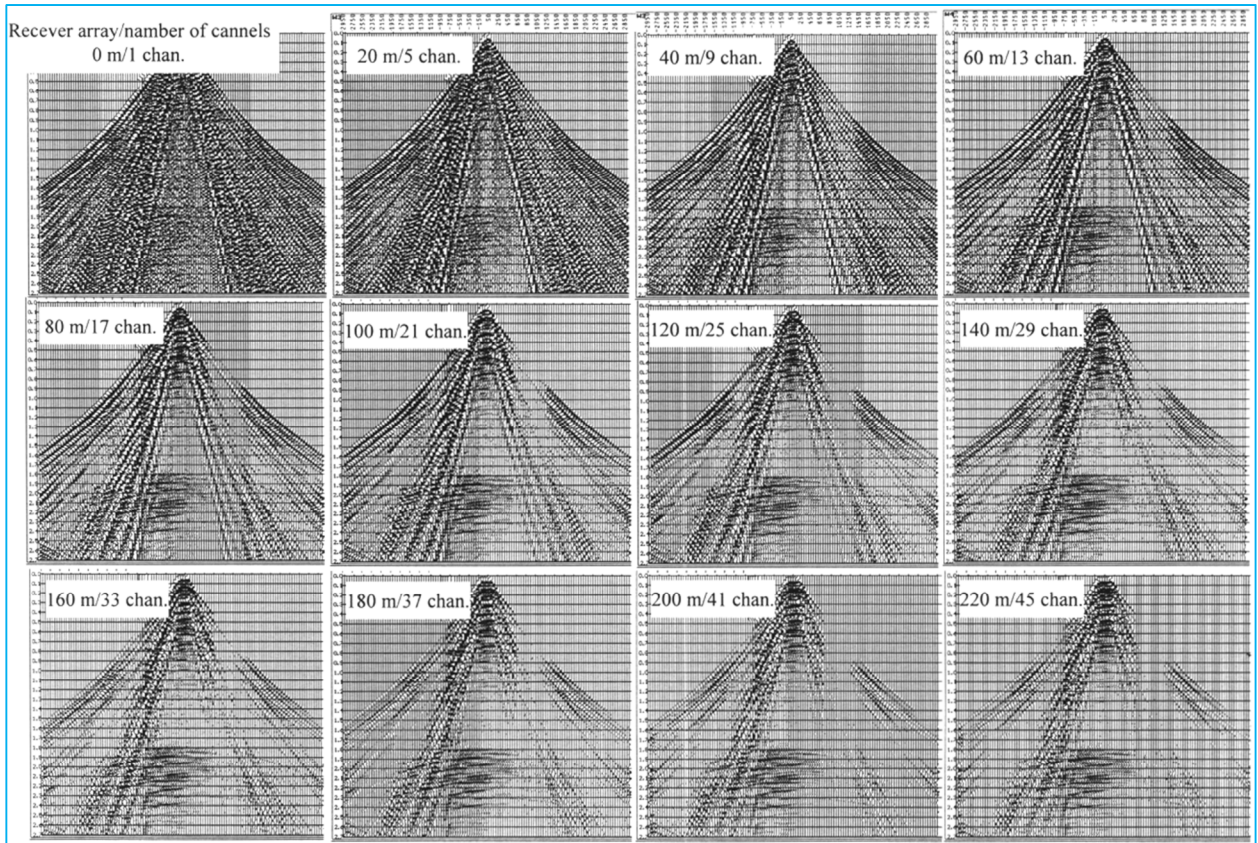
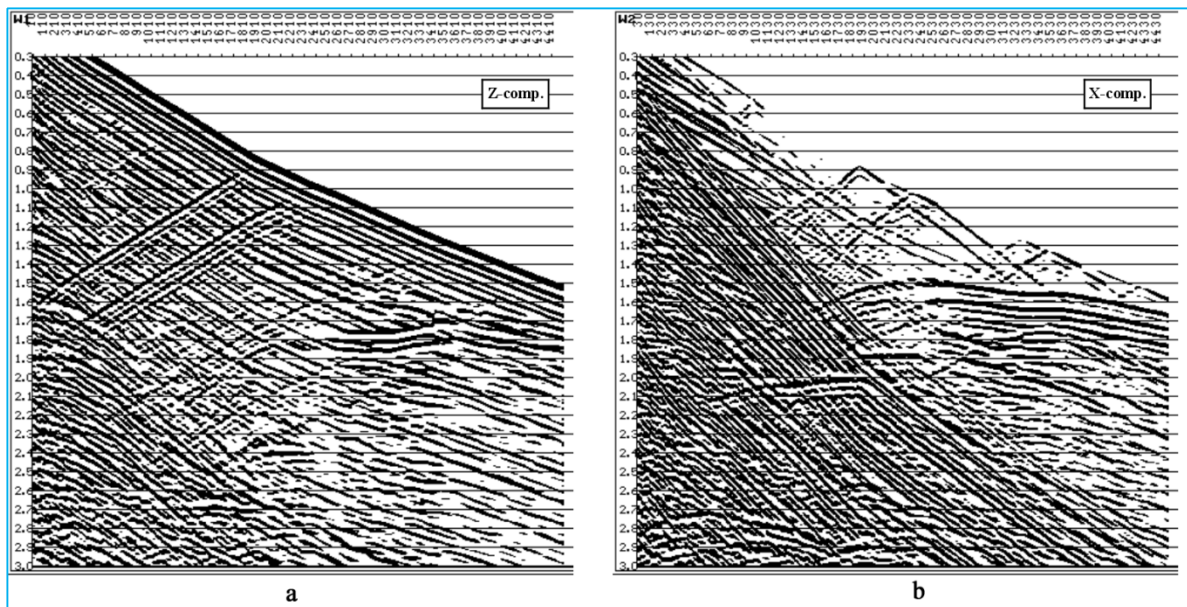


Fig.18. Model of the upper part of the cross-section (fragment).



**Fig.19.** Fitting of the receiver grouping bases for the central scheme of observations (medium elastic model).



**Fig.20.** Synthetic VSP shotgather (elastic medium model).

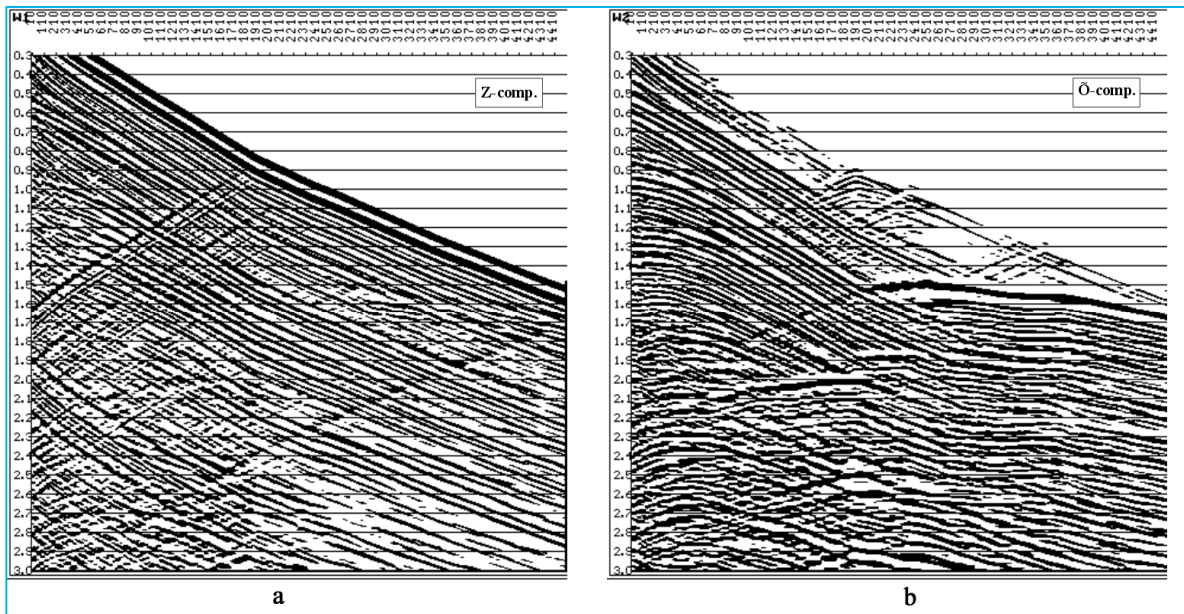


**Fig.21.** Synthetic VSP shotgather (acoustic medium model).

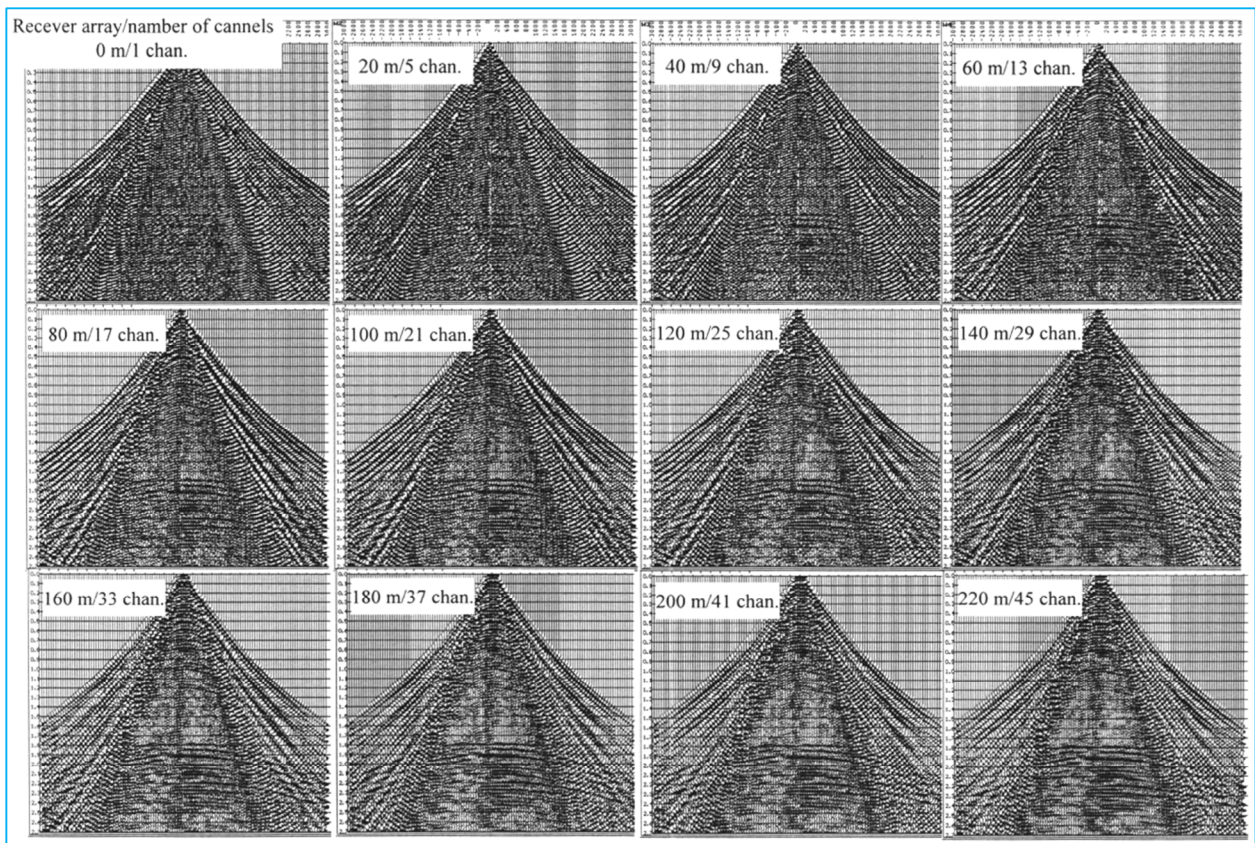


**Fig.22.** Fitting of the receiver grouping bases for the central scheme of observations (medium acoustic model).

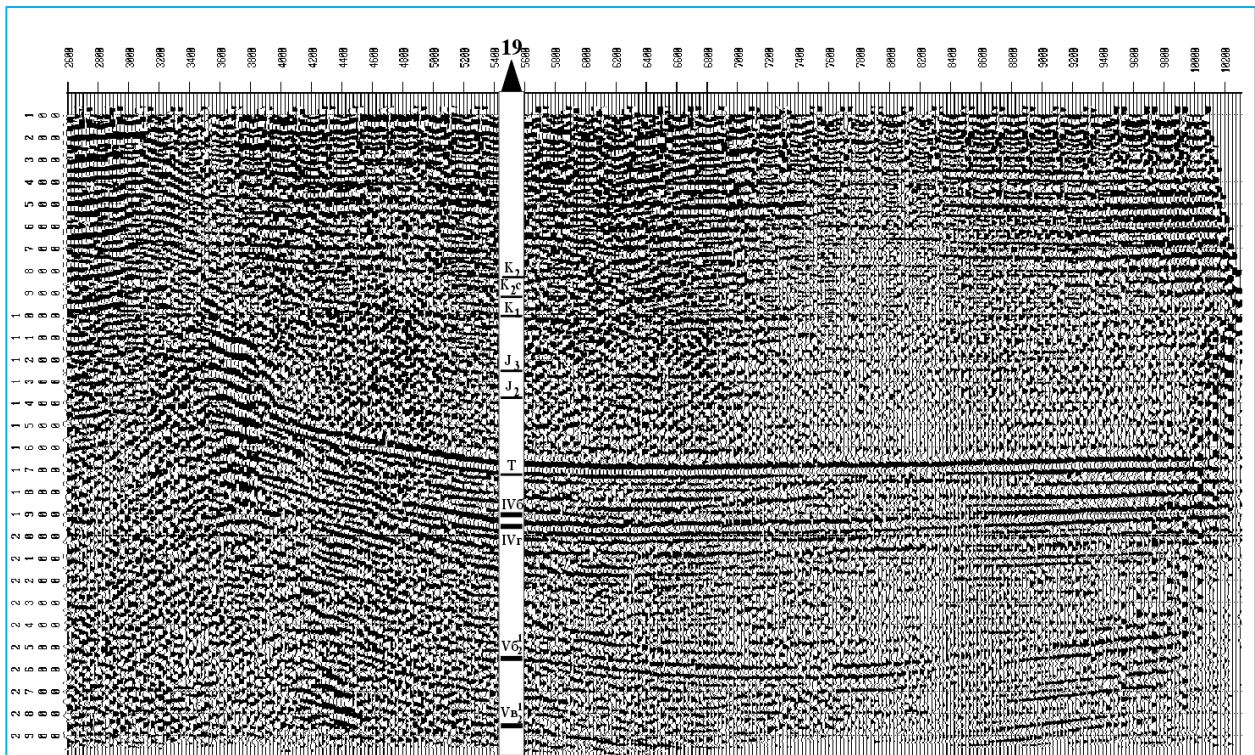


**Fig.23.** The modeled time cross-section, obtained with the central scheme of observations with the receiver grouping on the base  $l_G=150$  m and interval between the group centers  $DX_{RP}=50$  m

### 3 Studying of the near salt dome deposits

... connected with sub-vertical reflecting discontinuities, applying to the study of the near salt dome deposits, fault disruptions, zones of epigenetic changes in the rocks etc.

Hydrocarbon deposits in the near salt dome zones are quite important practically in all regions of the world. Main traps in them are tectonically screened, and screens there can be as salt bodies, as well as, multiple disruptive faults, complicating the near salt dome zones. Character feature of the near salt dome deposits is their narrow attribution to the screens (salt body or corresponding fault). Their exact tracing is necessary in this case. In this situation modeling can be very helpful, done with the *Tesseral* package, which has a number of major advantages over other ways of modeling.

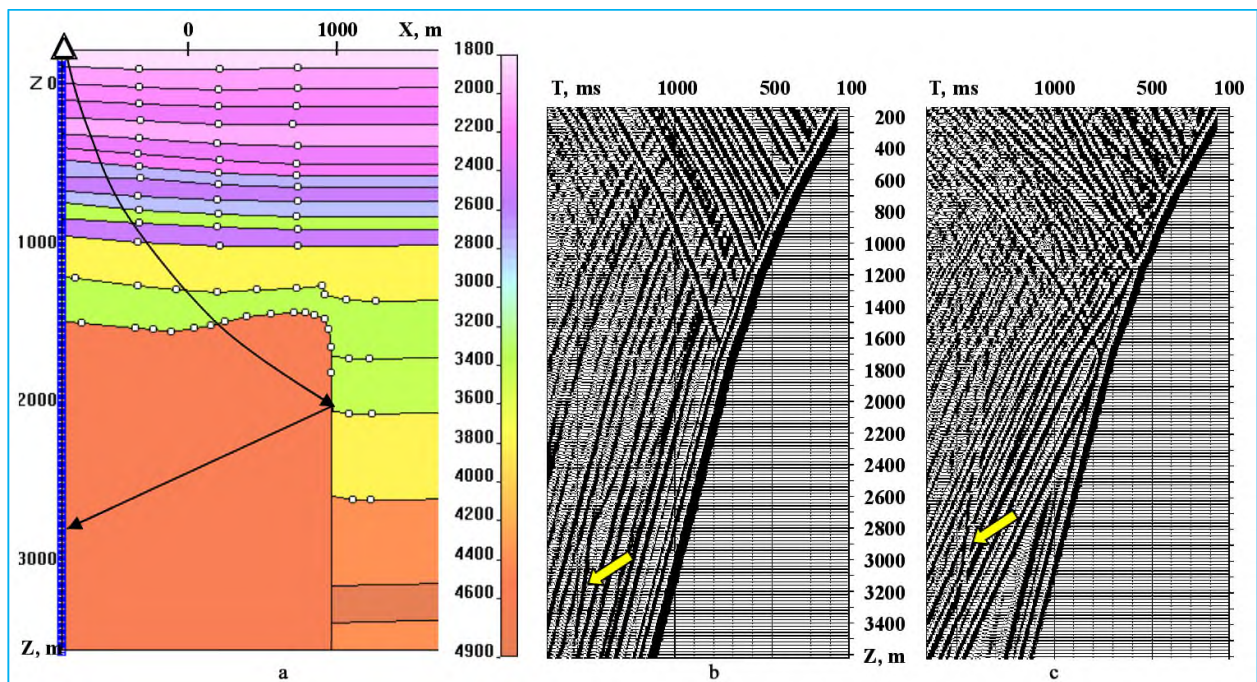
Consider two possible types of hydrocarbon screening by salt. The first type is relating to the trap screening by the sidewall of the salt dome, and in this case, the screen represents itself by a subvertical discontinuity, created by the salt body and the near deposits. The second type is relating to the traps, screened by the salt peaks, cornices etc. The characteristic feature of those traps is that the collector, as a rule, is placed in steeply inclined near salt deposits, overlaid by the peak salt. The boundary between the collector and the cover, although, is not characterized by the considerable angle of inclination, nevertheless, as a rule, is faintly expressed and poorly distinguished in the wave field.

Examine the possibilities of the *Tesseral* package of wave field modeling in indicated above conditions. The main objective for surveying of the traps of the first indicated type – is seismic tracing of subvertical reflecting boundaries. The principal complication is that, the produced reflections are descending, i.e. are propagating downward, and on the surface are not registered. At VSP those waves can be registered. In fig.24a is shown a model, formed in the

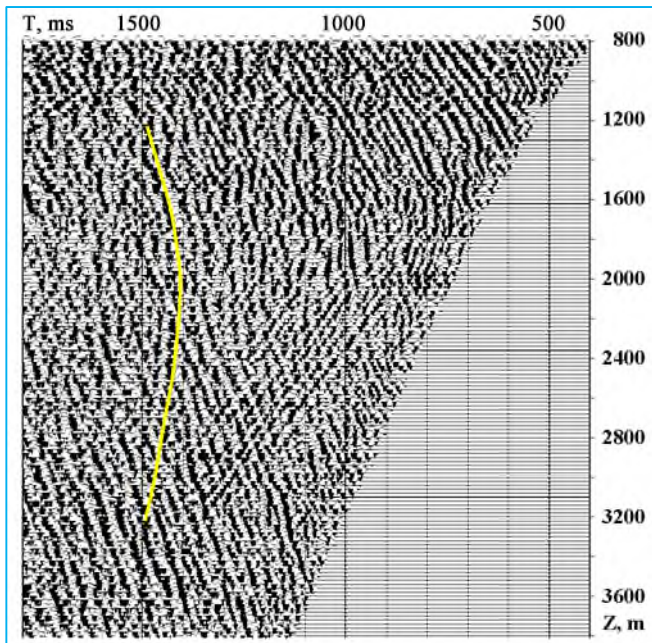
near area of the Rozumovsky-9 well (Andreyevsky salt dome, Dneprovsky-Donetsk Depression). Schematically shown with arrows, are ray traces for waves reflected from the wall of the salt dome and registered in the well. In fig.24b and fig.24c are shown correspondingly Z- and X-components of the synthetic wave field. As it can be seen from shown shotgathers, compressional waves, reflected from the dome wall (in figures they are marked with arrows), are quite well traced, especially in the X-component of the wave field (fig.24c).

Fig.25 shows the Z-component of the wave field registered in the Rasumovsky-9 well. In the indicated figure the field of the incident waves was subtracted. In the shotgather the arrow is showing the wave reflected from the dome wall. Its position and intensiveness is corresponding quite well to those obtained with the modeling. It is important to note that with those VSP shotgathers seismic images can be formed (migrated cross-sections) of the salt bodies [10]. The role of the *Tesseral* package in this case – is maximally optimizing the migration procedure that by many objective causes frequently becomes unstable.

Despite the big importance of the problem considered above, more significant is the creation of the subvertical discontinuity images by surface observation data. Such images are formed by the waves (more complex in kinematic relation) which on the way to the source – receiver have at least two reflections: from subhorizontal (further SH) and subvertical (further – SV) boundaries. Such waves bear the name of the duplex ones; by many researcher’s data [11,12], they are characterized by energy, sufficient to be distinguished from hindrances and reflections from SH discontinuities.



**Fig.24.** Modeling of reflection from the salt dome wall at VSP observations: a – source model (prototype of Andreyevsky salt dome, Dnieper-Donetsk Depression); b and c – VSP shotgathers for X- and Z\_ components correspondingly.



**Fig.25.** VSP shotgather (observed) with subtracted field of incident waves.

Attempts to trace the real material of the SV contacts emerge the questions: in what degree are reflections from such contacts dynamically expressed in the wave field, are the duplex reflections really produced in concrete conditions, what are polarizing properties of waves reflected from SV contacts etc. To solve those questions the *Tesseral* package can be quite appropriate. For example, in difference from the ray-tracing methods, there is no need of creation of the special program procedures, because this package models all types of waves, including the duplex ones.

An example of reflections from SV discontinuities by modeling can be seen on the analogue of the real cross-section of the Andreevsky salt dome and nearby to it a complex of terrigene deposits (central part of the Dnieper-Donetsk Depression). The velocity model is shown in *Fig.26*. Simulated are the observations by scheme of multi-overlay profiling with parameters: number of channels –60, step between the receiver points (RP) – 50m, step between shot points (SP) – 100m, RP disposition – central, maximal overlay –15.

*Tesseral* program is applied in the variant of wave field modeling for elastic mediums. As a result a set of CSP shotgathers is obtained.

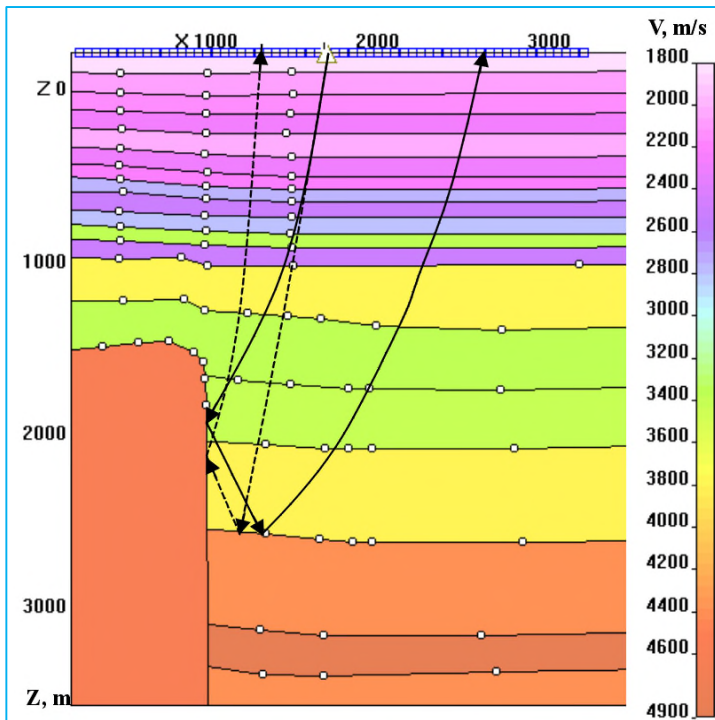


**Fig.26.** Source model (prototype- Andreevsky salt dome, Dnieper-Donetsk Depression).

In *Fig. 27 and 28* are shown examples of the time sections and Z-component of the wave field. Their combined analysis allows tracing characteristics of propagation of different wave types, which are generated for this model. In *Fig.27* is clearly seen creation and propagation of the duplex reflections with the ray trajectories: SP-SV discontinuity – SH boundary – RP, and SP-SH boundary – RP. The front of the duplex reflections, generated by SV discontinuity and located at 2600m depth SH boundary, in the figure is marked with arrows. Duplex waves in kinematic relation are recognized on the background of other waves in shotgathers, i.e. are confidently fixed on the observation surface.

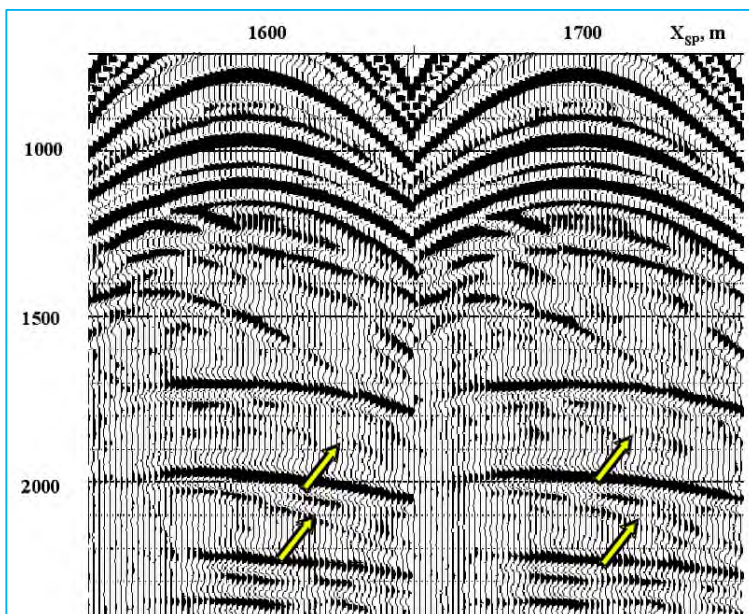


**Fig.27.** Snapshots of the wave field propagation (with arrows are shown the duplex reflections, generated on highlighted boundaries).

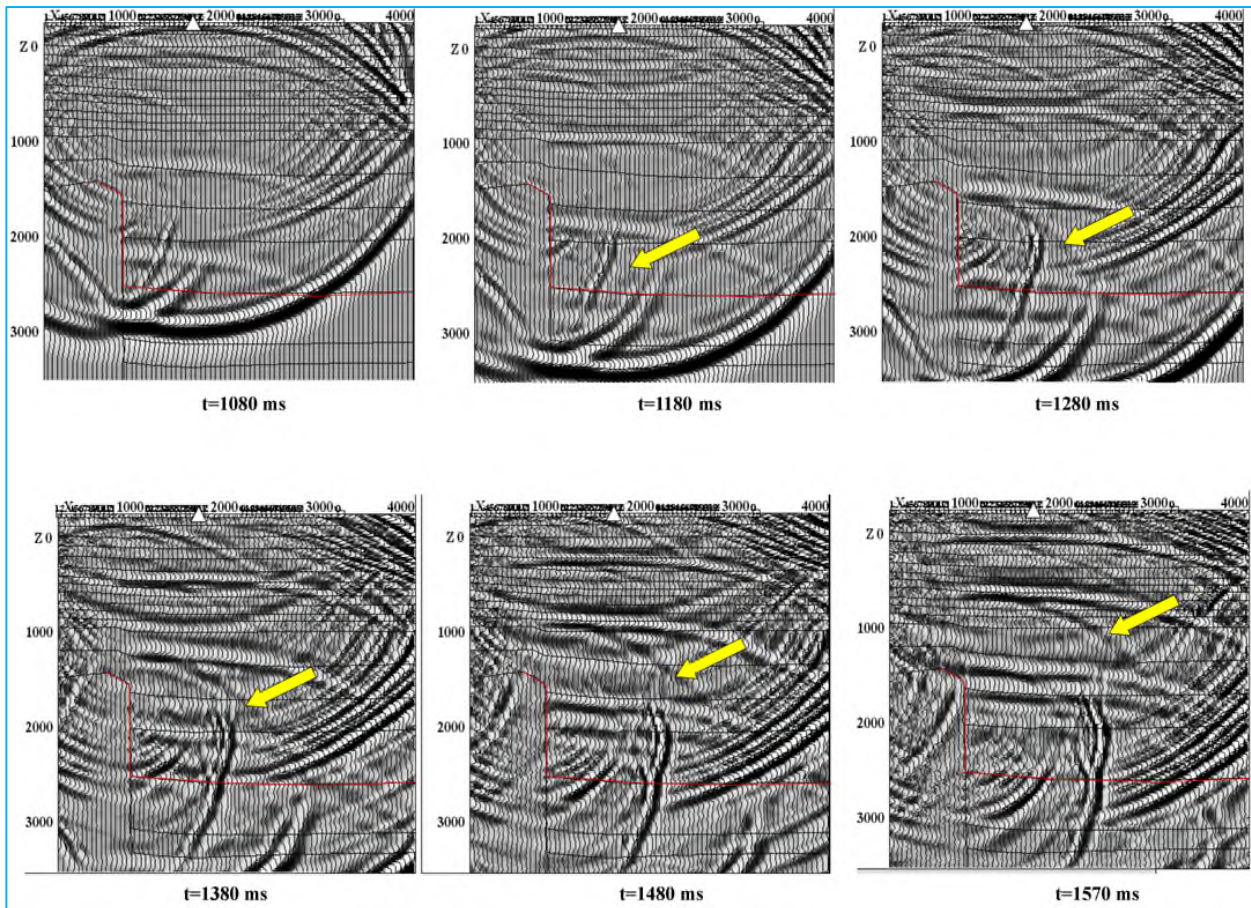


**Fig.28** Synthetic CSP shotgathers (with arrows are shown the duplex reflections).

The seismic image (migrated cross-section), obtained as a result of the shotgathers is processed with the conventional algorithm of the depth migration and is shown in *Fig.29*. With its help the sidewall of the dome can be predicted only approximately – by indication of breaking of tracing of the layered clastic deposits boundaries.

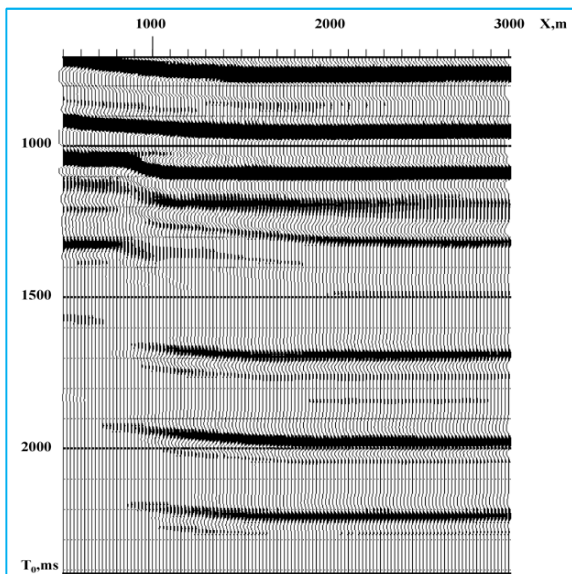


**Fig.29.** Seismic image by the migration transformation data for shotgathers of simple reflections.

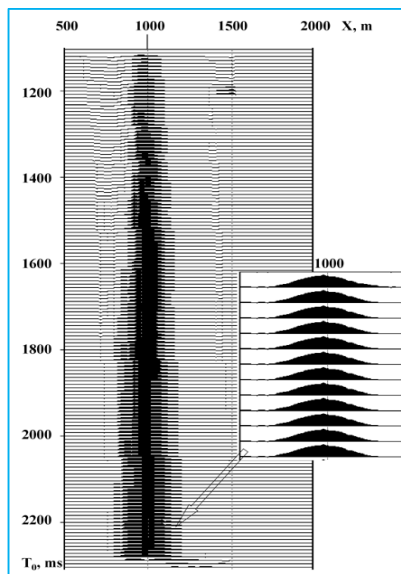


**Fig.30.** Seismic image by the migration transformation data for shotgathers of the duplex reflections.

In result of the duplex waves migration [12], an image of the salt dome side wall (**Fig.30**) is obtained. Its position exactly corresponds to the modeled one – X=1000m, that is an additional proof of the high precision of modeling of complex wave effects.

Comparison of the real near dome migrated cross-sections of subvertical discontinuities with the modeled ones, allows not only an increase in confidence in the obtained results, but also the correction of parameters of the migration procedures, for example the velocity characteristics of the cross-section.

Shown below is the example of the Starosangarsky salt dome, situated in the south part of the Dnieper-Donetsk Depression. Application of the *Tesseral* package is useful in increasing the effectiveness of prospecting of near dome traps of the second indicated type(under peak).

The model of the indicated salt dome is shown in **Fig.31**. Modeled reflecting horizons were given as the boundaries of division of macro-stratigraphic complexes. To define the velocity characteristics available well information was used.

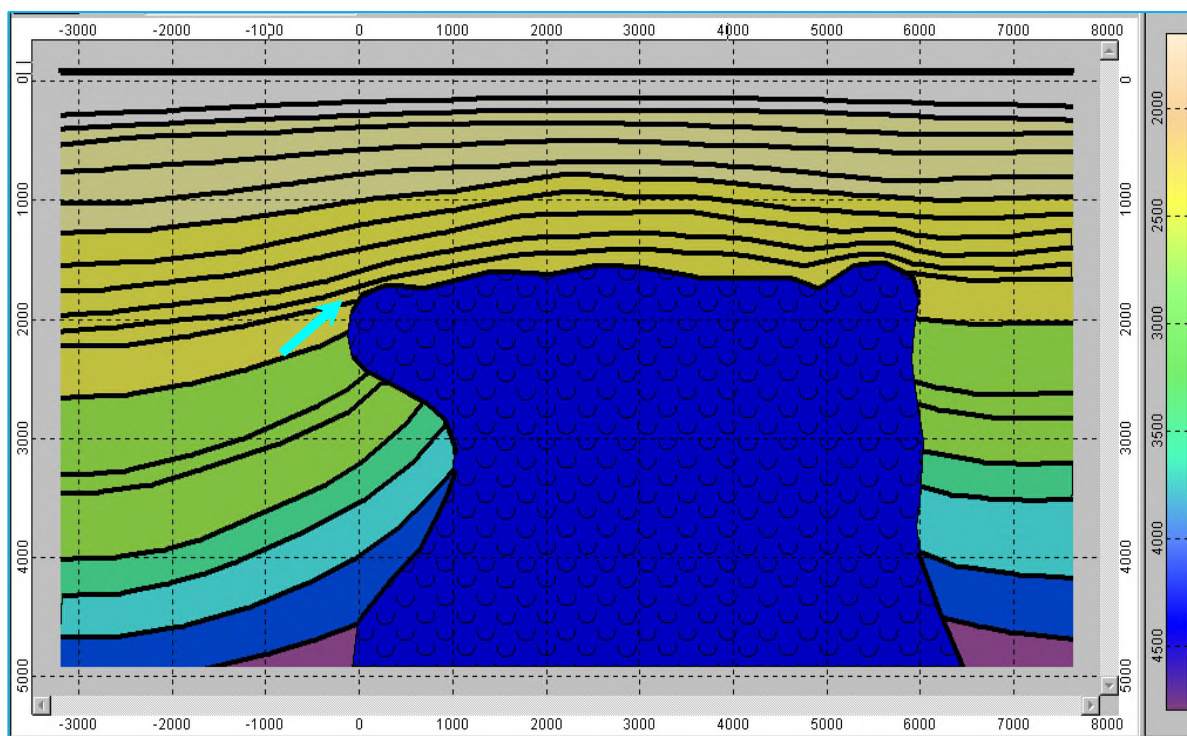


**Fig.31.** Model of the salt dome, built with the *Tesseral* package.

As it can be seen from the model, one flank of the salt diapire has cornice, and the second one is subvertical. Arrows in the figure show the survey object in deposits of the Low and Mid Carbon, with big angles of inclination coming under the salt dome cornice. Angles of inclination, defined by kern in the under cornice zone are 70°-80°.

For modeling of effects, occurring at the salt dome flanks the “exploding reflectors” mode was used, which allows the modeling of time cross-sections for the seismic waves, propagating normally from given horizons for the indicated intervals of inclination angles. Signal frequency was 30Hz. Modeling was done on the notebook PC Pentium II-500 with main memory 128 Mbytes.

On the model (**Fig.31**) with thicker lines are shown the horizon intervals generating seismic energy, and in **Fig.32** – the time cross-section, obtained as a result of “exploding reflectors” modeling.

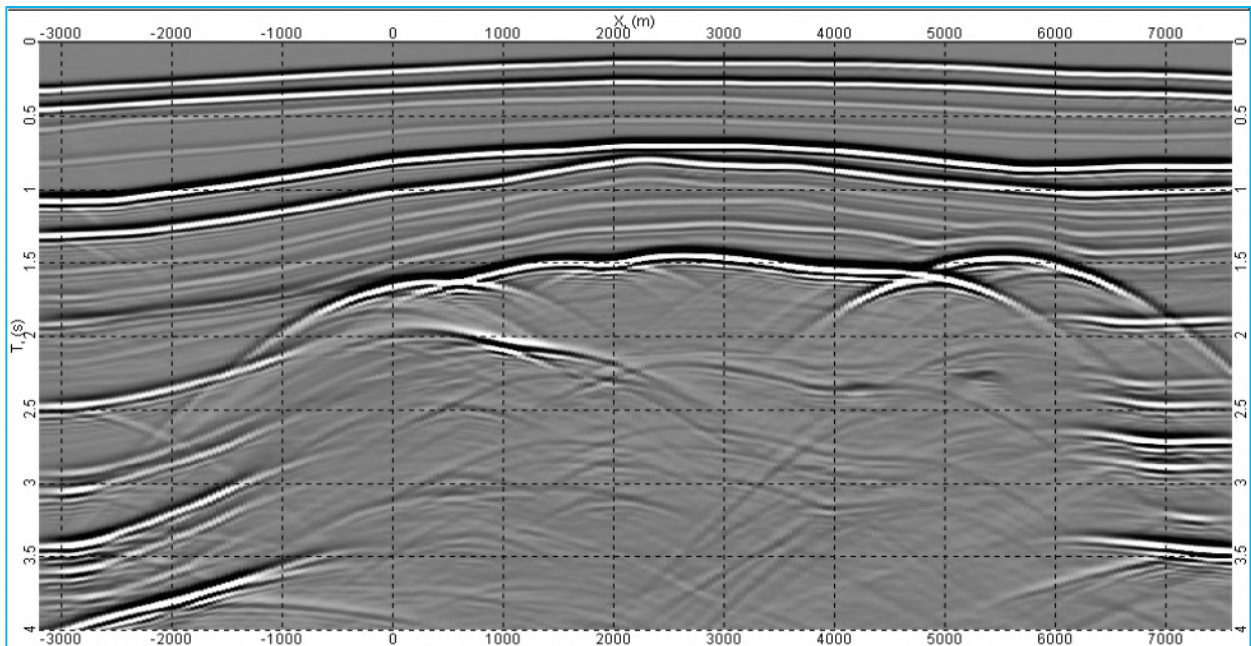


**Fig.32.** The time cross-section, obtained with the *Tesseral* modeling package.

The modeled time cross-section was processed with full-wave finite-difference post-stack migration (**Fig.33**). A characteristic feature of the seismic image obtained, is the practical absence of “pulling” into the salt of subhorizontal reflecting boundaries in the right part of the dome, and also a comparatively low level of migration noises, that proves right dynamic correspondences of reflected and diffracted waves.

On the whole it can be stated a good correspondence of the model (fig.31) and the obtained seismic image (**Fig.33**), except steeply risen parts of under peak deposits. The synphasis axes, observed inside the salt dome, are formed by multiple waves and in real conditions can be falsely interpreted.

To see in detail the process of propagation of the wave field though the cornice of the salt dome a sequence of snapshots was taken (fig.34), which allows visualization of a clear reflection from the bottom of the cornice (shown with arrow in the last snapshot). To generate snapshots modeling of the CSP shotgather was used. The system of observations had the following parameters: central disposition, minimal offset – 40m, maximal offset – 3000m, interval between receivers – 40m, sampling step 2ms.

Tracing with snapshots of the wave, reflected from the bottom of the salt cornice, allows the definition of the intervals of offsets from the shot point, for which it comes to the surface, and by this way, calculation of the optimal length of the receiver line is possible.

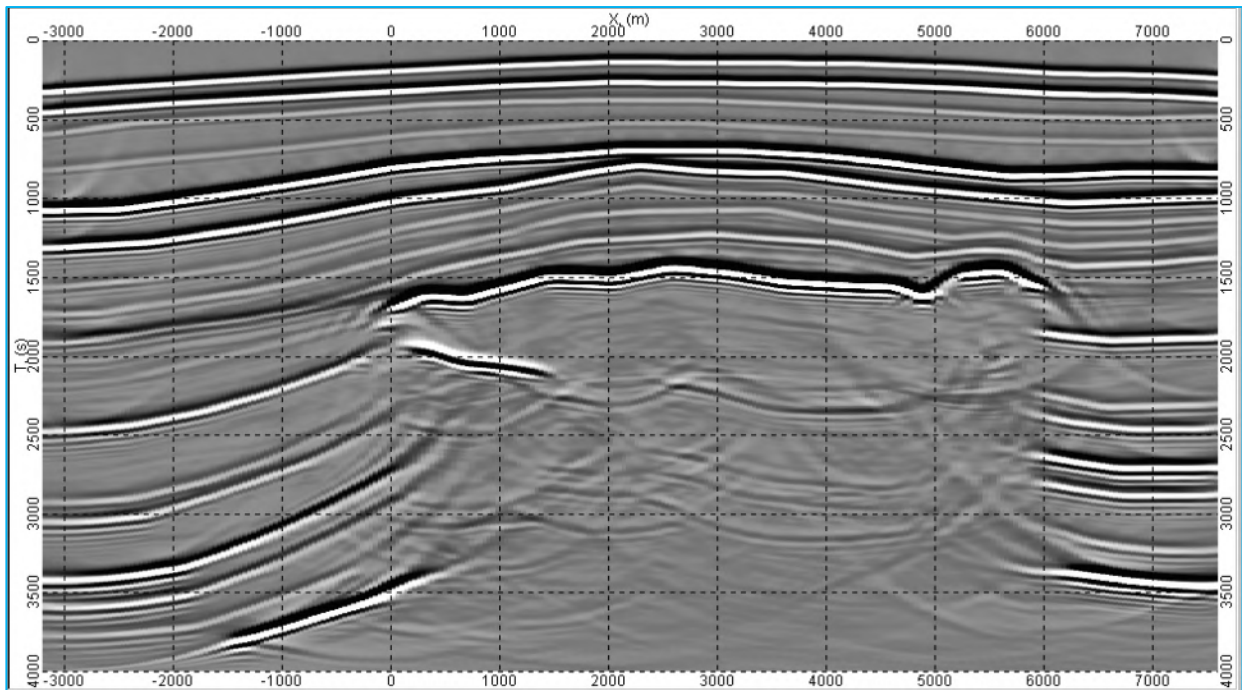


**Fig.33.** Seismic image, obtained with post-stack migration of the model time cross-section.

On the basis of the analysis of the obtained modeling results (fig.32 34) and modeling data processing (fig.33) there can be stated the following methodically important results:

1. The bottom of the salt peak is traced quite definitely, because it is a contrast velocity discontinuity. On it the inversion of velocity of waves propagation occurs, that is why this under salt horizon is characterized by the signal phase inversion, that can be a diagnostic indication of the presence of the salt cornice and consequently, a possible under salt trap of hydrocarbons.
2. The salt top boundary is a powerful multiple-creating seismic discontinuity, from which are observed packs of multiple and partly multiple waves. In particular, multiple waves from the salt top, complicated by partly multiple waves, can be erroneously interpreted as sub-salt deposits. That is why in seismic-geological conditions of crypto-diapire tectonics obligatory procedure of the data processing must be multiple wave attenuation.
3. The obtained time cross-section (fig.32) can be used for testing of the migration procedures, importance of which becomes obvious, if take into account such essential differences, which are observed between the time cross-section (fig.37) and the migrated time cross-section (fig.33).
4. Modeling and the duplex waves migration transformations of for the studying of small-blocking tectonics, in particular, in the thin-layered thicknesses.

Actuality of studying such objects is known: disruptive dislocations (including small-amplitude ones) and allocated to them zones of epigenetically changed rocks, can similarly to the salt bodies, be effective screening elements of the hydrocarbon deposits of the structure-tectonic type.

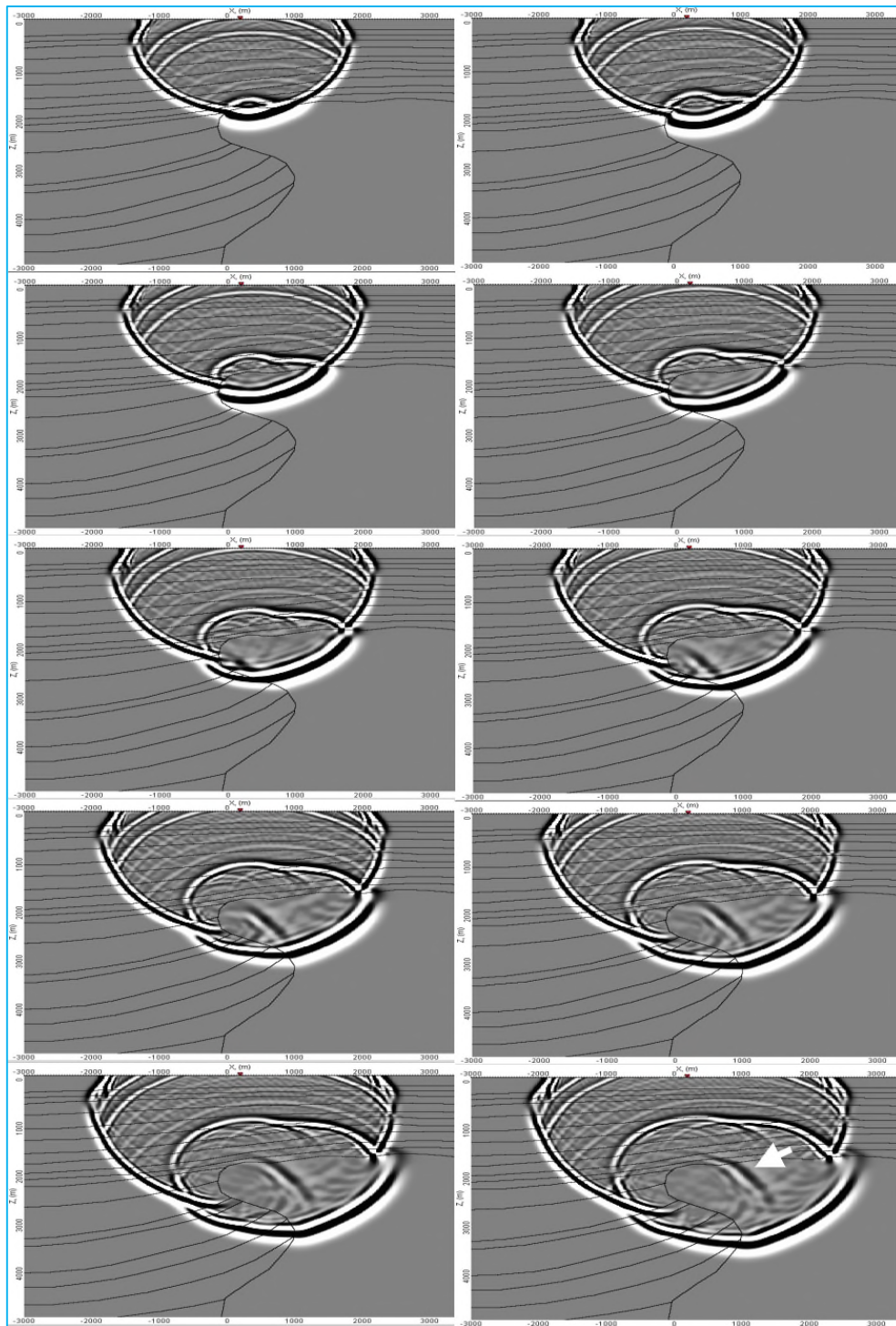


**Fig.34.** Subsequent phases of passage of the wave field through the salt dome cornice (with arrow is shown the wave, reflected from the bottom of the salt cornice).

In the practice of seismic prospecting small-blocking tectonics (faults with amplitude of 10-15m), occur in insignificant breaches of the discontinuities phase correlations. Such correlating dislocations in mid-horizon (thin-layered) thicknesses, as a rule are very unreliable. To this, the lithology changes along the boundary, leading to the phase change, which can be erroneously taken for the fault dislocation. In the same time, the duplex waves, forming on the strong (basic) subhorizontal boundary can be an indicator of the fault dislocation in the mid-horizon thickness. Today's accumulated experience of modeling and migrational transformations of the

duplex waves proves, that it is, as a rule, an effective tool for studying and solving such fine problems. See the modeling example.

For obtaining quantitative estimations of the duplex wave intensity in the mid-horizon thickness, a model was used representing an interchange of layers with 10m thickness and with compressional wave velocity (P - waves)  $\alpha_1 = 2000$  m/s and  $\alpha_2 = 4000$  m/s, shear wave velocities (SV - waves)  $\beta_1 = 1150$  m/s and  $\beta_2 = 2310$  m/s and densities  $\rho_1 = 2.01$  g/cm<sup>3</sup>  $\rho_2 = 2.35$  g/cm<sup>3</sup>. Thin-layered pack with thickness  $h = 1150$ m underlies homogeneous medium with velocities  $\alpha_3 = 5000$  m/s,  $\beta_3 = 2900$  m/s,  $\rho_3 = 2.5$  g/cm<sup>3</sup>. The boundary between thin-layered pack and homogeneous medium was used for the duplex waves migration as the basic one. This model was complicated with reflecting discontinuity, which was modeled as a layer with 50m thickness, crossing thin-layered medium almost orthogonally and having P-wave velocity 3000m/s.

**Fig.35** shows the result of modeling where: a) – the source model of the cross-section; b) – the obtained modeling shotgathers (Z – component), in which with arrows are shown the duplex waves; c) – the time cross-section (CDP); d) – the seismic image, obtained with conventional procedure of the shotgathers depth migration; e) – the seismic image of the target subvertical element of the cross-section, which was obtained by the application of specialized procedures of the shotgathers migration for duplex reflections.

As it can be seen from the given example, within the thin-layered pack are formed the interference waves [5], having the resonance character. The last one has visible synphases axes that are not tied to any of the thin-layered pack boundaries. In the time cross-section (fig.35c) and the seismic image (**Fig.35d**), within the thin-layered pack, are forming weak boundaries, which do not have the phase shift sufficient to identify the dislocation. At the same time, in the seismic image obtained with the duplex waves (fig.35e), subvertical discontinuity is identified unambiguously and in full correspondence with the given model.

It must be noticed, that breaking of the resonance conditions, caused by the layering changing, variations of LVZ (low velocity zone, weathered layer) etc, can be erroneously taken for a fault, and, in the same time, the true low-amplitude dislocation can be skipped.

In **Fig.36** for the model similar to the considered above, are shown conditions of the resonance breaking, caused by insignificant (first degrees) inclination of a thin-layered pack, which begins from coordinate  $X=1600$  m. The synthetic shotgathers in the zone of the broken resonance (**Fig.36b and 36c**) within the thin-layered pack lose the regularity, which can be observed in the resonance zone (**Fig.36a**). In the time cross-section (**Fig.36e**) breaking of the resonance conditions is shown in a sharp change of the seismic record pattern, accompanied with the phase shifts, which can be erroneously taken for the small-amplitude disruptive dislocations.

So, the *Tesseral* package provides wide possibilities for modeling of wave effects, connected with the variable in scale fault tectonics, and also allows differentiation among them by their form effects.

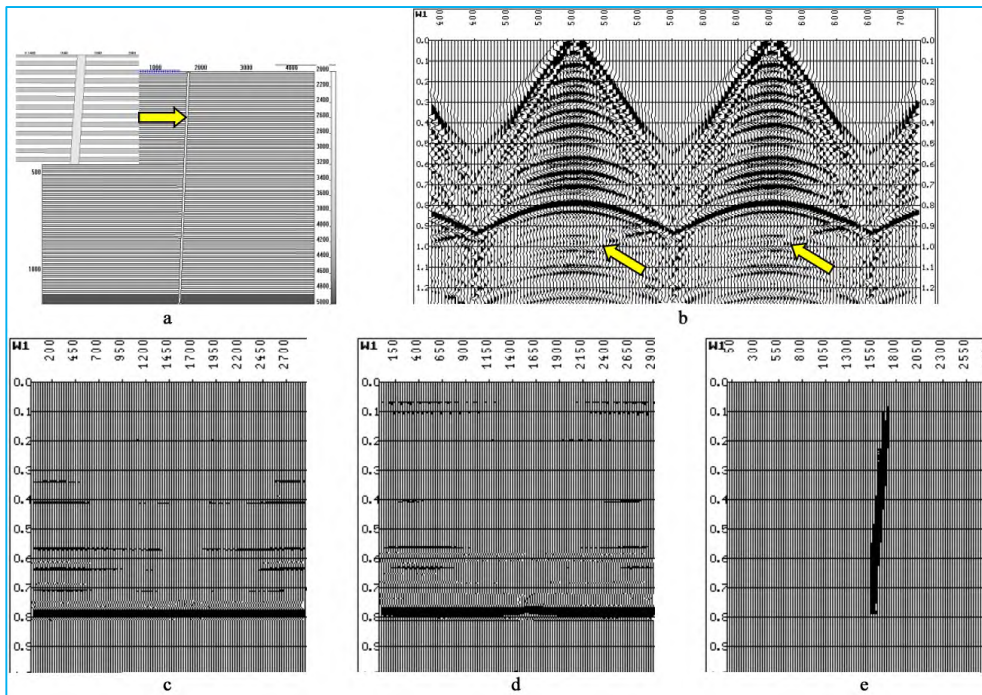


**Fig.35.** Modeling of sub-vertical low-amplitude dislocation in the thin-layered pack (a-, b-, c-, d-, e – explained in the above text).

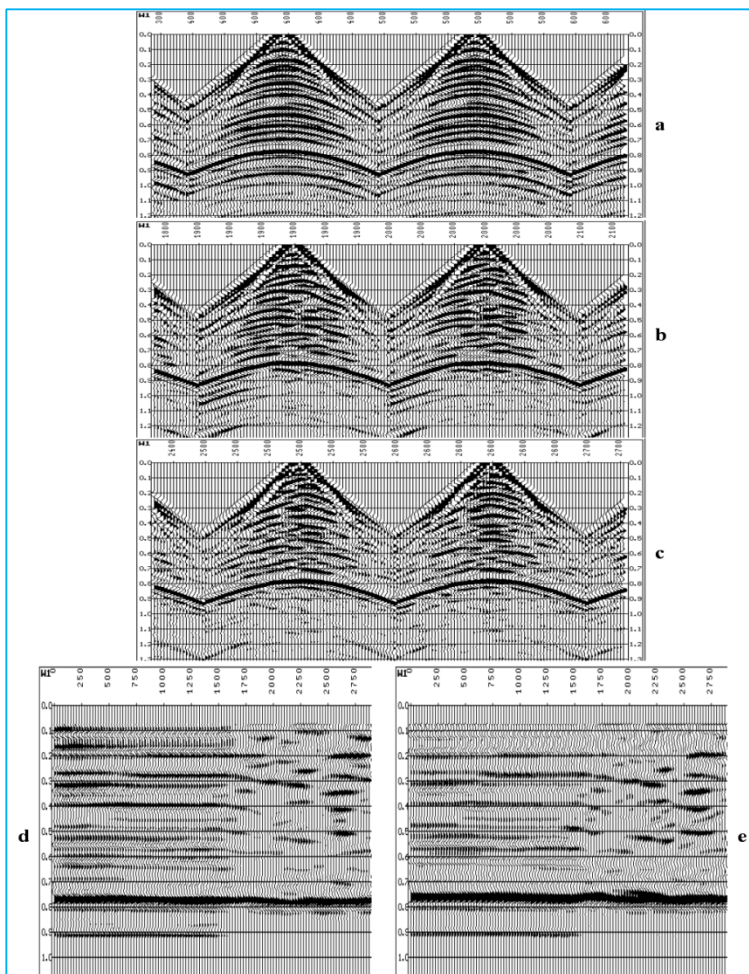


**Fig.36.** Modeling of the resonance wave effects in the thin-layered medium (a-, b-, c-, d-, e – see explanations in the above text).

## 4 Testing of the seismic data processing programs

... processing parameters, tuning and testing of new processing procedures.

One of the most important problems in seismic survey data processing is program testing. New algorithms and programs are tested with the aim of ascertaining their functional possibilities, as well as old ones, for example in transition to new survey areas, new geological problems appear. As a rule, testing is done on real materials, which is also a necessary processing stage. However, in conditions of uncertain geological structure, which always occurs even in well-studied sites, the testing stage, connected with usage of modeling data is necessary, and as we suppose, must be preceding all other types of testing.

In section 3 in the example of modeled time cross-sections the importance of migration in studying the near dome deposits was shown (fig.32 and fig.33). The migrational procedures, as a rule, require detailed testing, because their various types react differently on the transformation aperture value, frequency band of the seismic record, range of the boundary inclination angles, diffracted waves etc. In this aspect the *Tesseral* package can be widely used, taking into account its potential of shotgathers and the time cross-section modeling. A possibility to impose an irregular noise on the modeled wave fields even more approximates the modeling result to a real field.

To illustrate the indicated option more examples of the *Tesseral* package application for algorithms and program testing are supplied.

### 4.1 Multiple waves subtraction with the Born dissipation rows.

A presently widely used algorithm of subtraction (attenuation) of multiple waves, reflected from the observation surface [13] is characterized by such important properties as, not requiring information about wave velocities and not setting restrictions on the medium structure. It provides opportunity to obtain shotgathers without multiple waves, i.e. subtraction occurs without applying the signal accumulation procedure in the space of the time cross-section.

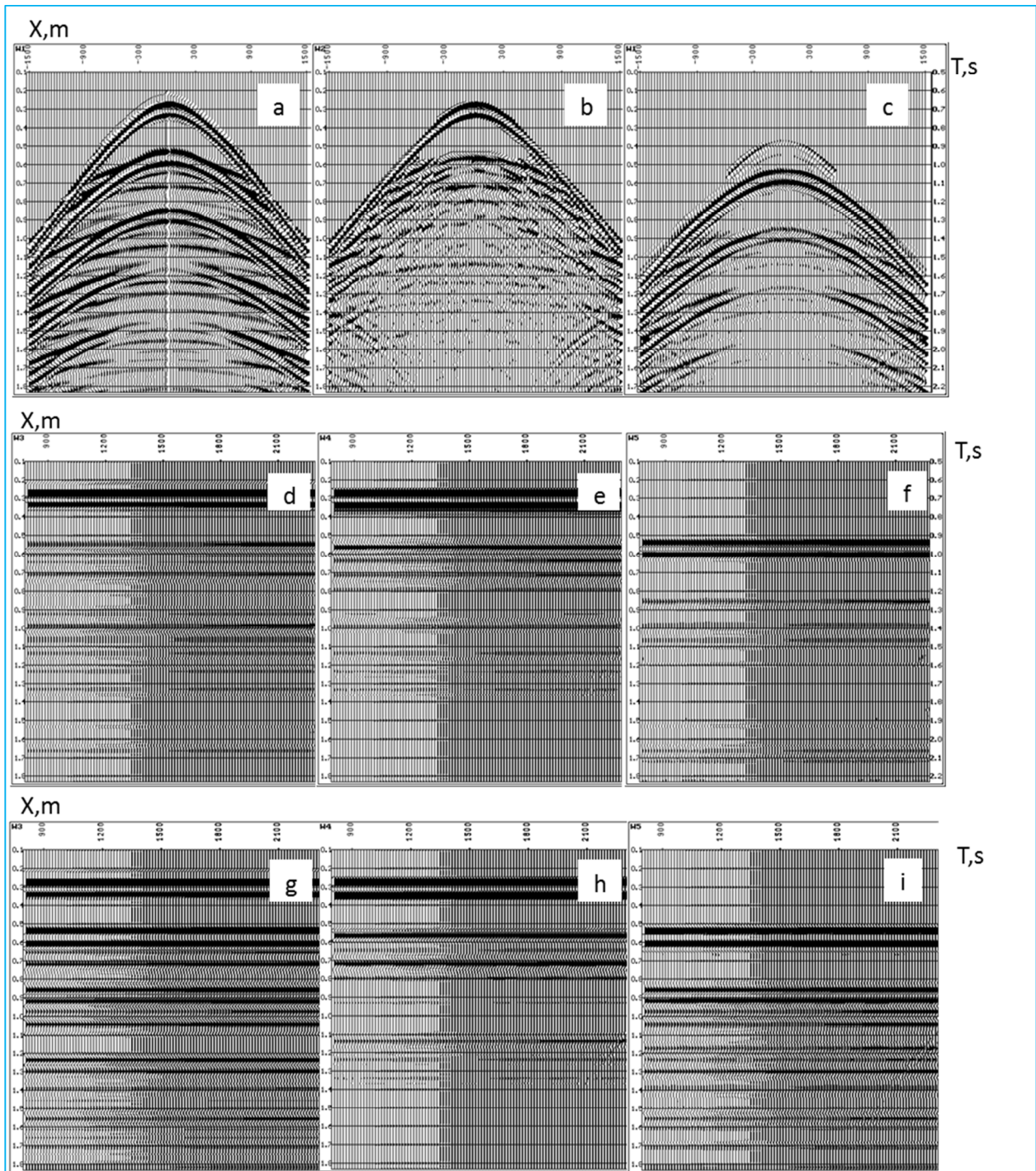
For modeling, a horizontally layered medium model with 10 layers was used. Modeling was done in the acoustic approximation of the wave equation. Used for this model velocities are gathered in table 1.

Table 1

Layer number	Layer thickness H (m)	Compressional wave velocity V(m/ms)	Time in the time cross-section T (ms)
1	200	1500	266
2	400	2700	563
3	100	3600	619
4	150	3200	712
5	100	3800	764

6	620	3400	1132
7	200	4000	1232
8	220	4400	1332
9	250	5000	1464
10	$\infty$	5400	-

In fig 37a is shown CSP shotgather, obtained for the central observation scheme in the offsets interval [-1500m, 1500m], observation step  $\Delta X_p=15$  m.



**Fig.37.** Testing of the program of subtraction of multiple wave-hindrances, based on usage of the Born dissipation rows:

a – initial CSP shotgather;

b – CSP shotgather after multiple wave subtraction ;

c – multiple waves shotgather;

d – the time cross-section before multiple waves subtraction;

e - the time cross-section after multiple waves subtraction;

f – the time cross-section of multiple waves;

g – the partial time cross-section (48 nearer channels) before multiple waves subtraction;

h - the partial time cross-section after multiple waves subtraction;

i - the partial time cross-section of multiple waves.

of shot points  $\Delta X_s=15$  m, number of channels – 201, frequency 30 Hz. In fig.37b – the shotgather after application of multiple waves subtraction and in fig. 37c – the multiple waves shotgather.

In **Fig.37d, e, f** respectively show the time cross-sections without subtraction of multiples, with subtraction of multiples and the time cross-section of multiple waves.

In the cross-section with subtracted multiples (**Fig.37e**) there are practically no multiple waves connected with the surface. At the same time, in the cross-section, which was formed without subtraction (fig.37d), their intensiveness is quite big. Also are seen in the time cross-section synphasis axes, connected with multiple waves, which have significant intensiveness. In this case the effectiveness of the CDP summation for the suppressing of multiple waves is insufficient.

The possibility of multiple wave subtraction before summation, plays an important role for procedures, operating with the seismic wave amplitudes in shotgathers, or small bases of summation, for example at AVO. The biggest complexity in this appears in the nearer channels, where effectiveness of suppression of multiples at accumulation on a small base is the lowest. In fig.37 *g, h, i* the time cross-sections are shown, obtained for the nearer 48 channels (magnitude of offsets  $\pm 360$  m), correspondingly without procedure of the multiples subtraction, with applications of this procedure and the time cross-section of multiple waves. From the indicated figures it is clear, that after the procedure of multiple wave subtraction of the time cross-section, obtained with the small base (fig.37h), almost do not differ qualitatively from that obtained with the full base. Those cross-sections differ only by intensiveness of the synphasis axes, which refers mainly, to AVO-effect presented in this case. In the same time, cross-sections, obtained with full or partial bases, without the procedure of multiple wave subtraction, differ quite significantly as by intensiveness of the synphasis axes, as well as by their quantity.

## 4.2 Effect of the procedure of multiple wave subtraction on the velocity analysis

Intuitively it is clear, that lowering the level of the regular hindrances (multiple waves) must positively influence the velocity analysis, but how much this methodical approach is effective in each concrete case, remains unknown. In this situation the role of modeling is crucial.

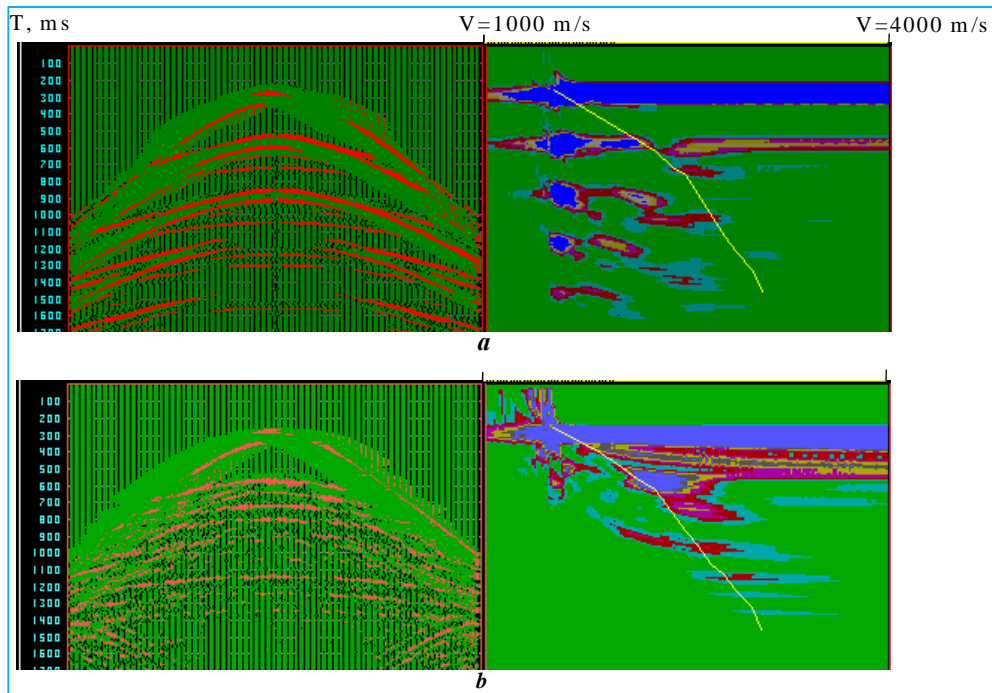


**Fig.38.** Testing of influence of the multiple waves subtraction procedure on the velocity analysis:

a – primary CSP shotgather and corresponding to it velocity specter;

b – CSP shotgather with subtracted multiples and corresponding to it velocity specter.

In **Fig.38a, b** are shown CSP shotgathers (for a horizontally layered medium it is an analogue of CDP shotgathers) with corresponding velocity specters in variant without subtracting of multiples (**fig38a**) and with subtracting of multiple waves (**Fig.38b**). In the velocity specters (**Fig38a and Fig38b**) the average velocity dependency on time  $t_0$  is shown with a broken line. Before the multiple wave subtracting the main expansion after time  $t_0=0.7s$  is located to the left of the average velocities line, i.e. velocities defined in the result of the velocity analysis, appear lower the average, that contradicts the given thick-layered medium model. At the same time, after the multiple wave subtracting (**Fig.38b**) practically all the expansions are located to the right of the average velocity line, which is fully consistent with the model.

Indicated testing could not be done on the basis of real material, because the thin-layered quasi-anisotropic real media may have variants, when effective velocities are lower than the average, that would not allow to reach correct conclusions about the influence of interference of once-reflected and multiple-reflected waves on the velocity analysis.

### 4.3 Programs of attenuation of the surface hindrance-waves

In the practice of data processing for attenuating the surface waves are used different F-K filters and other means, using difference in apparent velocities of useful and surface waves. See the example of the effectiveness of application of the program of subtraction of the surface waves by the Lu algorithm [14], based on the singular decomposition.

In **Fig.39** are shown fragments of the time cross-sections, obtained from model, shown in **Fig.17**.

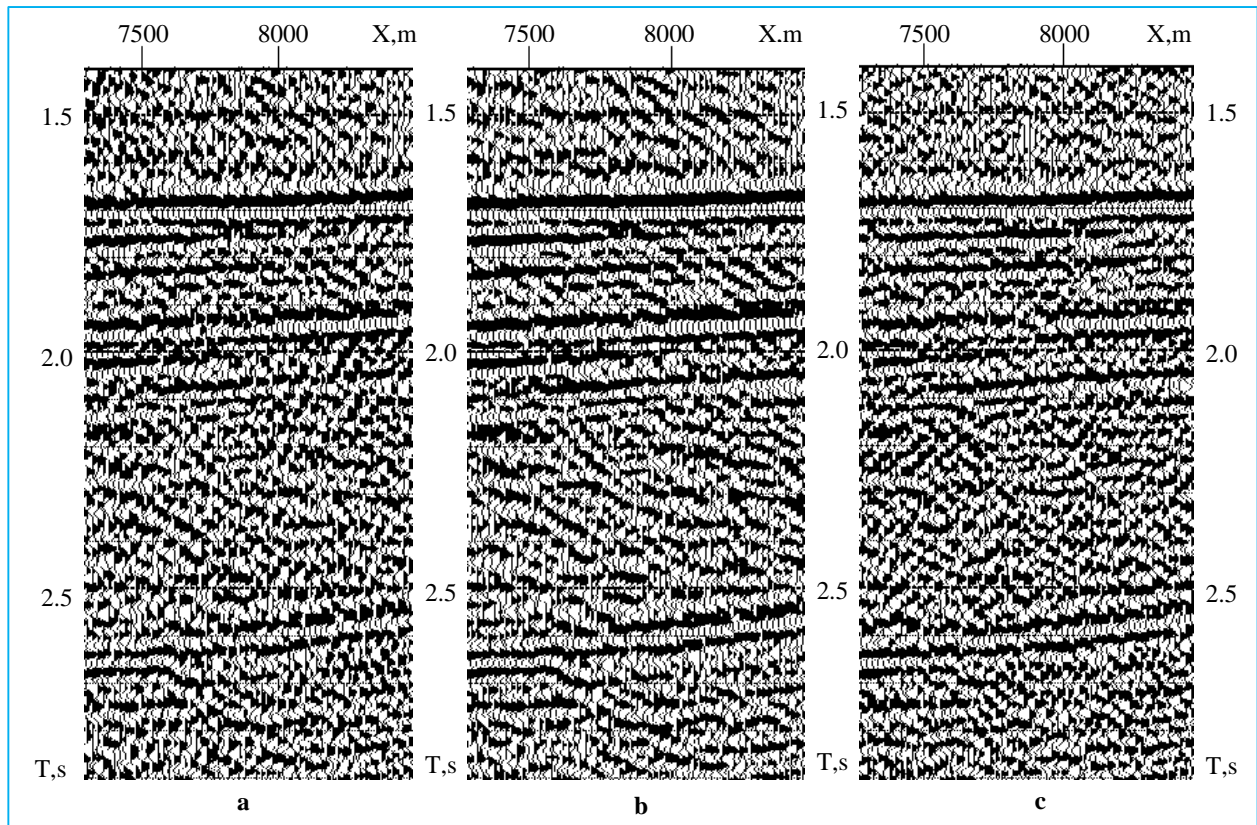


**Fig.39.** Testing of programs of attenuation of surface hindrance-waves:

a – time cross-section without suppression to surface hindrance-waves;

b – cross-section with suppression of surface hindrance-waves on the basis of F-K filtration;

c- cross-section with suppression of surface hindrance-waves based on singular decomposition.

In this case for modeling the flank system with overlay number  $S=12$  was used. Fig.39a shows the time cross-section without application of the procedure of subtraction of surface hindrance-waves, in fig.39b – the time cross-section, obtained with usage of F-K filter, and in fig.39c – the time cross-section, obtained with the tested procedure of the surface wave subtraction, based on singular decomposition. As it is seen with comparison of indicated pictures, in the interval of coordinates  $X=7500\text{m}-8000\text{m}$ , on times  $t_0=2.1\text{s}-2.5\text{s}$  in fig.39a and 39b (without subtraction and F-K filtration) intensive curved synphasic axes are observed, not corresponding to the model used. In the condition of an unknown geological structure, they can be erroneously taken as elements of the angle of discrepancy in mid-horizon thickness. At the same time, an application of the tested algorithm allowed a sharp reduction of the aforementioned mentioned hindrance.

#### 4.4 Survey layout parameters and AVO processing

AVO-analysis is applied for the surface observation data and, as a rule, it is necessary to operate not with dependency of the reflection coefficient on the incidence angle of the wave, but with dependency of the amplitude on the incidence angle.

Using *Tesseral* package in every concrete case provides possibility to estimate inaccuracy, introduced in AVO by such substitution. To this aim, the package allows estimation of the wave amplitude not only on the observation surface but at any point in the medium.

Because amplitudes of incident waves can be estimated as well as reflected ones, there appears to be a possibility to estimate the reflection coefficient for every target discontinuity, and also, to estimate the effects of the wave passage through the medium.

Consider for better evidence the widely cited in literature, Ostrander model [15]. It reflects literally observed correspondences of parameters of clays, gas- and water-saturated sandstone, applicably to non-deeply bedded deposits.

The model is characterized by following parameters:

Gas-saturated sandstone -  $\alpha_1=1967\text{m/s}$ ,  $\beta_1=1311\text{m/s}$ ,  $\rho_1=2.05\text{g/cm}^3$ ,  $\sigma_1=0.1$ ;

Water-saturated sandstone -  $\alpha_2=2131\text{m/s}$ ,  $\beta_2=0.87\text{m/s}$ ,  $\rho_2=2.1\text{g/cm}^3$ ,  $\sigma_2=0.4$ ;

Clay -  $\alpha_3= 2177\text{m/s}$ ,  $\beta_3=0.888 \text{ m/s}$ ,  $\rho_3=2.16\text{g/cm}^3$ ,  $\sigma_3=0.4$ . Here  $\sigma$  – Poisson coefficient.

Fig. 40 shows a theoretical curve  $R(\vartheta)$ , obtained by Zoepritz formulae, and a curve of dependency  $A(\vartheta)$ , where  $R$  – reflection coefficient,  $A$  – amplitude of wave reflected from the boundary between gas-saturated and water-saturated sandstone, obtained as a result of modeling with the *Tesseral* package,  $\vartheta$  – angle of incidence of the wave on the boundary. Amplitude in this case is a velocity of the displacement of the wave field vertical vector. As it can be seen from the picture, those curves differ. It is caused by not taking into account of the effect of the wave passage, which in the case of a homogeneous half-space, is reduced to the geometric divergence, and angle of the dependency of amplitudes.

Expression for the cylindrical wave potential, and exactly such wave is modeled in 2-D case, is:

$$\phi(r, t) = \frac{1}{\sqrt{r}} f\left(t - \frac{r}{c}\right),$$

where  $\phi(r, t)$  – cylindrical wave potential,  $r$  – radius,  $c$  – velocity of wave propagation. Taking above into account, Z-component of the displacement vector of the wave field can be expressed as:

$$\frac{\partial \phi}{\partial Z} \approx \frac{i\omega \cos \varphi}{c\sqrt{r}} e^{-i\omega \frac{r}{c}}.$$

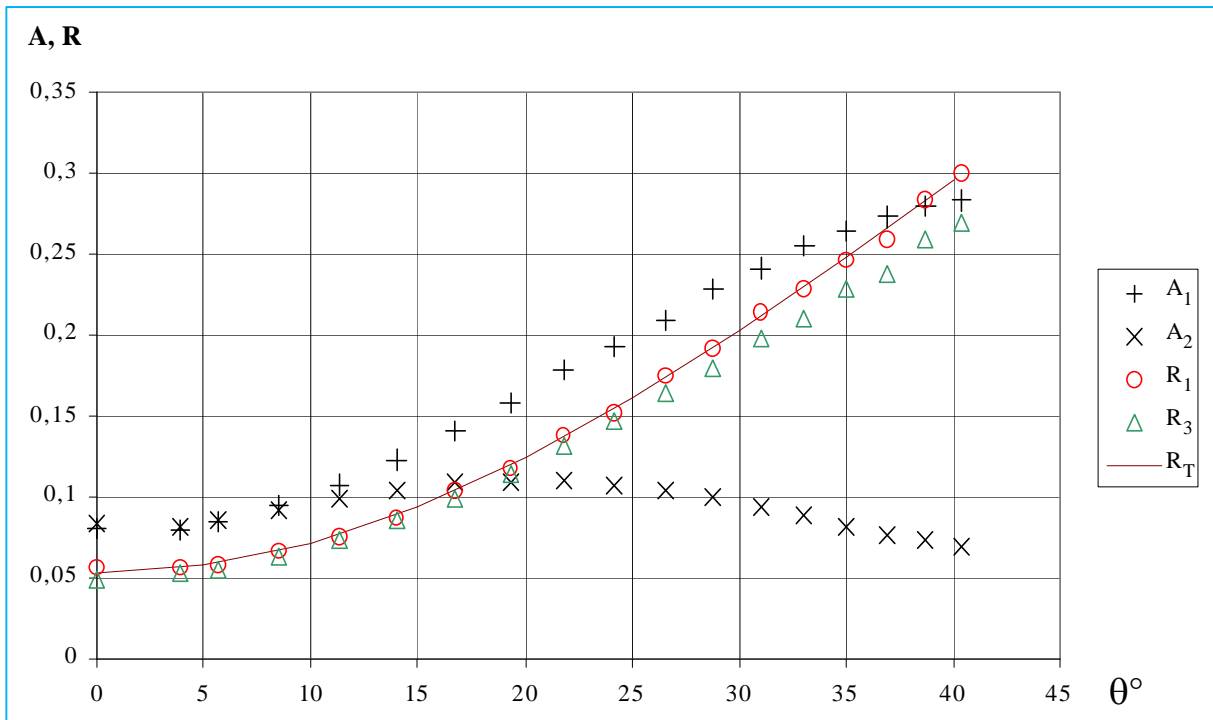


**Fig.40.** Dependencies of AVO-amplitudes of reflected waves and reflection coefficients for gas-water contact. Legend:  $A_1$  – amplitude of Z-component of the field of particle displacement for realization of grouping at receiving;  $R_1$  – reflection coefficient of synthetic shotgather for gas-water contact in condition of two-layered medium model;  $R_2$  – reflection coefficient of synthetic shotgather for gas-water contact in condition of three-layered medium model;  $R_T$  – theoretic reflection coefficient.

Here appears explicit dependency of amplitude from angle  $\varphi$  (angle of inclination of the wave front towards the horizontal direction) that is necessary to define to obtain the reflection coefficient normalization of the reflected wave is used, the incident along the same ray that excludes angle dependency. The *Tesseral* package for this aim, as was indicated, provides the possibility of measuring wave amplitudes not only at the receiving points, but also at any point within the medium.

In practice, in condition of the existence of the developed low velocity zone (weathered layer), dependency of amplitude of Z-component of the wave field vector displacement from the angle of wave propagation is attenuated, because in this case measurement of the observation surface value is close to the full displacement vector. But this is possible only with the condition of the absence of the angle of dependency of amplitudes from the direction of the sources and receivers: the last one is distorting as Z-component, as well as, full vector of the wave field displacement.

**Fig.40** shows the curve of the amplitude dependency from the angle of wave incidence, obtained after the application of the receiver grouping procedure. Here angle dependency is characterized by additional multiplier  $\cos^3 \varphi$ , which practically obliterates the presented AVO-effect, caused by the jump of the Poisson coefficient on the discontinuity.

Introduction of necessary corrections for divergence and angles of wave propagation allows obtaining correct values of AVO-dependency, which for the considered model is shown in **Fig.40**. Analogous dependency of amplitudes from the angle is proper not only for the case of cylindrical wave, but also for a spherical one, which has important practical significance.

Similar to the above modeling use, correspondence of the medium parameters, when on the discontinuity of water-saturated and gas-saturated sandstones compressional wave velocity and density is diminishing, and velocity of shear waves is increasing, this can be observed in many literary sources. Such dependency is observed on the contact cover – collector, for example, clay with indicated above parameters – gas-saturated sandstone. In the same time, contrast of parameters on the boundary of water-saturated sandstone – clay is practically absent, and reflection from it in the wave field, obtained for the three-layered model, consisting from gas-saturated sandstone and a 20-meter layer of water saturated sandstone, underlain by clays, is not observed. But an AVO curve in relation to the two-layered model is changing (see fig.40 curve  $R_3$ ), and those changes in some cases reach 10% of the reflection coefficient.

The above case shows significant influence of thin layering on AVO, which significantly diminishes the possibilities of AVO-interpretation methods, based on application of linearized Zoeppritz formulae and other apparatus, and also, on a thick-layered medium model. In the same time, in indicated conditions the role of the full-wave modeling arises to the level of the basic method of AVO-analysis.

The considered examples of the program testing and the processing parameters tuning can be widened applicably to the problems of each individual user. To this aim the *Tesseral* package provides wide and flexible opportunities.

## Summary

Examples shown in this Methodical Manual encompass only a small portion of possible areas of application for the *Tesseral* package.

As indicated, each individual user forms the scope of problems to be solved using the package.

For example, for VSP, considering specifics of the full-wave equation, it is possible with modeling to solve the following problems in practically all seismic effects in an elastic medium:

1. Realization of two-component wave receiving.
2. Seismic model realization in conditions of transversally isotropic media (physically anisotropic or quasi-anisotropic).
3. Unlike ray-tracing methods here without distortions are modeled effects, connected with incidence of the discontinuity of waves under wide angles (close to critical or overcritical). It allows obtaining non-distorted wave picture in conditions of remote shot points at non-transversal VSP. At this, data can be modeled for conditions of receiving oscillations in deviated (even horizontal) wells and sources on the surface or inside wells.
4. Package provides the possibility of correct modeling of resonance wave effects in a non-monotonous thin-layered pack, which allows obtaining a correct understanding about characteristics of seismic waves in a mid-horizon area, including false resonance waves of significant intensiveness.
5. Taking into account effects of quasi-anisotropic thin-layered non-monotonous thicknesses, allows corrections to be made in the absorption decrements, which are defined by the velocity dispersion within the frequency band, used at VSP and SL (sonic logging).

6. Modeling of effects, connected with sub-vertical reflecting discontinuities, including the duplex waves of different types and polarization.
7. An important advantage of the Tesseral package at VSP is the possibility of wave identification. Wave identification is easily done with analysis of a series of wave field snapshots  $t=\text{const}$ , which can be obtained with any discreteness. On these snapshots it is possible to trace position and way of propagation of every wave pack, beginning from the moment of its appearance to its exit on the surface. At this, snapshots can be presented as X-, Z-components, and also as a full displacement vector.
8. Additionally to the indicated opportunity of identification of shear waves it is possible to use a combination of VSP shotgathers, obtained in elastic and acoustic approximation. Because in the latter case shear waves are not modeled, they cause all types of differences in shotgathers.
9. There is a possibility to exclude multiple waves reflected from the surface. For example, reverberational, i.e. to obtain VSP shotgathers with reverberation and without it, which is important at marine seismic surveys and onshore surveying with a complex LVZ (low velocity zone, weathered layer) structure, when it is necessary to define part of waves-satellite generated in the upper part of the cross-section.
10. Within the *Tesseral* package realization of wave field modeling for the frequency band and technique of the acoustic well logging execution, there exists the possibility of excitation of compressional and shear waves.
11. A separate problem is the realization of cross-well observation, which can serve as a basis for the estimation of precision of tomographic images of mid-well area.
12. Specially realized in the package is the possibility of amplitude measuring not only in the receiving points, but in any place of the cross-section. This presents convenient means for AVO-analysis, allowing to take into account the influence of the discontinuity curvature, thin-layering, anisotropy etc on AVO-effect, obtained, in particular, by VSP data.
13. In the package is the possibility of modeling of wave dissipation on small-, medium- and large-scale heterogeneities, which is very important in VSP observations for the estimation of possible fluctuations of kinematic and dynamic parameters of incident and reflected waves.
14. An important feature of the package is the possibility of creation of mixed models, for example, for acoustic and elastic mediums. By this way conditions of marine observations can be simulated, when at wave generation in acoustic medium, the essential area of their propagation falls in the elastic medium.

A no less imposing list of example topics can be presented for the surface seismic surveys as well.

The package is in constant development and this methodical manual will be expanding in the future. It will include also concrete examples of uses for the package, (obtained by its different users) that will widen geography, as well as its methodical content.

## References

1. Wright J. The effect of transverse isotropy reflection amplitude versus offset. –Geophysics. – 1987.- V.52. – p.p. 564-567.
2. Banic N.C. An effective anisotropy parameter in transversely isotropik media. – Geophysics. – 1987. – V. 52. – p.p. 1654-1664.
3. Ryan-Grigor S. Empical relationships between transverse isotropy parameters and  $V_p/V_s$ : Implication for AVO. –Geophysics. – 1997. – V 62. – p.p. 1359-1364.
4. Nevskij M.B. Quasi-anisotropy of seismic waves velocities. Moscow: Science, 1974. –179 p.
5. Molotkov L.A., Smirnova N.S. To the problem of thin-layered pack oscillation between two elastic half-spaces. - In book: Problems of dynamic theory of seismic waves propagation T 11. – S.Peterbourg: PGU edition, 1971. – p.4-26.
6. №3. – c.110-115.
7. De G.S., Winterstein D.F., Meadows M.A. Comparison of P-and S-wave velocities and  $\theta/s$  from VSP and sonic log data. – Geophysics. – 1994. – V.59. – p.p.1512-1529.
8. Galperin E.I. Polarization method of seismic surveys. – Moscow: Nedra, 1977. – 277p.
9. Thomsen L., Weak elastic anisotropy:Geophysics. – 1986. – V 51. – p.p.1954 – 1966.
10. Marmalevsky N., Gornyak Z., Roganov Y., Khankin A. Migration of VSP data in presence of lateral velocity changes. – 60th EAGE Conference and Technical Exhibition. – Leipzig, 1998. – PO32.
11. Lutsenko B.N. Seismic waves interpretation within complex media. – Moscow: Nedra, 1987. – 120 p. (in Russian).
12. Marmalevsky N.Y., Gornyak Z.V., Roganov Y.V., Mershchiy V.V. Duplex waves migration transforming is the base of forming of subvertical geological boundaries Seismic imagies. – Scientific – technical conference “Geopetrol 2000”. – Krakow, Poland, 2000. – p.177 – 182. (in Russian).
13. Berkhout A.I. and Verschuur D.I. Estimation of multiple scattering by iterative inversion Part I: Teoretical consideration. – Geophysics, 62, pp.1586-1595.
14. Liu X. Ground roll suppression using the Karhunen –Loeve transform //Geophysics. - 1999. – 64, № 2. – p.564 - 566.
15. Yu G. Offset amplitude variation and controlled – amplitude processing. – Geophysics. – 1985. – V.50 . – p.2697-2708.